frontiers in Electronics

REVIEW
published: 13 May 2021
doi: 10.3389/felec.2021.685513

Motion Artifact Removal Techniques for Wearable EEG and PPG Sensor Systems

*Dongyeol Seok[1†], Sanghyun Lee[1†], Minjae Kim[1†], Jaeouk Cho[1] and Chul Kim[1,2]**

[1]*Biomedical Energy-Efficient Electronics Laboratory, Department of Bio and Brain Engineering, Korea Advanced Institute of Science and Technology, Daejeon, South Korea,* [2]*KAIST Institute for Health Science and Technology, Daejeon, South Korea*

Removal of motion artifacts is a critical challenge, especially in wearable electroencephalography (EEG) and photoplethysmography (PPG) devices that are exposed to daily movements. Recently, the significance of motion artifact removal techniques has increased since EEG-based brain–computer interfaces (BCI) and daily healthcare usage of wearable PPG devices were spotlighted. In this article, the development on EEG and PPG sensor systems is introduced. Then, understanding of motion artifact and its reduction methods implemented by hardware and/or software fashions are reviewed. Various electrode types, analog readout circuits, and signal processing techniques are studied for EEG motion artifact removal. In addition, recent in-ear EEG techniques with motion artifact reduction are also introduced. Furthermore, techniques compensating independent/dependent motion artifacts are presented for PPG.

Keywords: wearable devices, electroencephalography, photoplethysmography, motion artifact removal, EEG electrodes, digital signal processing, in-ear EEG, PPG artifact compensation

OPEN ACCESS

Edited by:
Woon-Hong Yeo,
Georgia Institute of Technology, United States

Reviewed by:
Chang-Hwan Im,
Hanyang University, South Korea
Youngjae Chun,
University of Pittsburgh, United States

****Correspondence:***
Chul Kim
kimchul@kaist.ac.kr

†These authors have contributed equally to this work and share first authorship

Specialty section:
This article was submitted to Wearable Electronics, a section of the journal Frontiers in Electronics

Received: *25 March 2021*
Accepted: *22 April 2021*
Published: *13 May 2021*

Citation:
Seok D, Lee S, Kim M, Cho J and Kim C (2021) Motion Artifact Removal Techniques for Wearable EEG and PPG Sensor Systems. Front. Electron. 2:685513. doi: 10.3389/felec.2021.685513

1 INTRODUCTION

Wearable devices have made significant progress in the field of health care, fitness, and diagnosis over the past few decades. Unobtrusive, user-friendly, and long-term usable fully integrated wearable systems enable healthcare devices to monitor the human body condition continuously and to give feedback to users (Dias and Paulo Silva Cunha, 2018). The advances of application-specific integrated circuit (ASIC) technology reduce the size of electrical devices, thereby increasing the availability of small-size devices in everyday life (Yin and Ghovanloo, 2007; Zou et al., 2008). In addition, recent substantial developments in computation algorithms and wide-bandwidth wireless communication technologies foster the everyday use of wearable devices (Aun et al., 2017; Beniczky et al., 2020). Especially in 2020, the World Health Organization (WHO) proclaims the COVID-19 pandemic, which increases the global demand for in-home patient monitoring based on the temperature, respiration rate, and blood oxygen content (Chamola et al., 2020; Hedayatipour and Mcfarlane, 2020). To get through this era, many researchers are currently proposing wearable biosensors as a solution to an epidemic prevention system against COVID-19 (Seo et al., 2020; Shan et al., 2020; Zhao et al., 2021; LifeSignals, 2021).

Figure 1 shows several kinds of the current wearable healthcare devices measuring various bio-signals such as electroencephalography (EEG), photoplethysmography (PPG), and electrocardiography (ECG). EEG devices in **Figure 1A**, mostly worn on a head, are utilized for attention training, sleep stage monitoring, machine controlling, and seizure detecting by analyzing human brain activity. PPG signals, especially used in the sports field to monitor the amount of

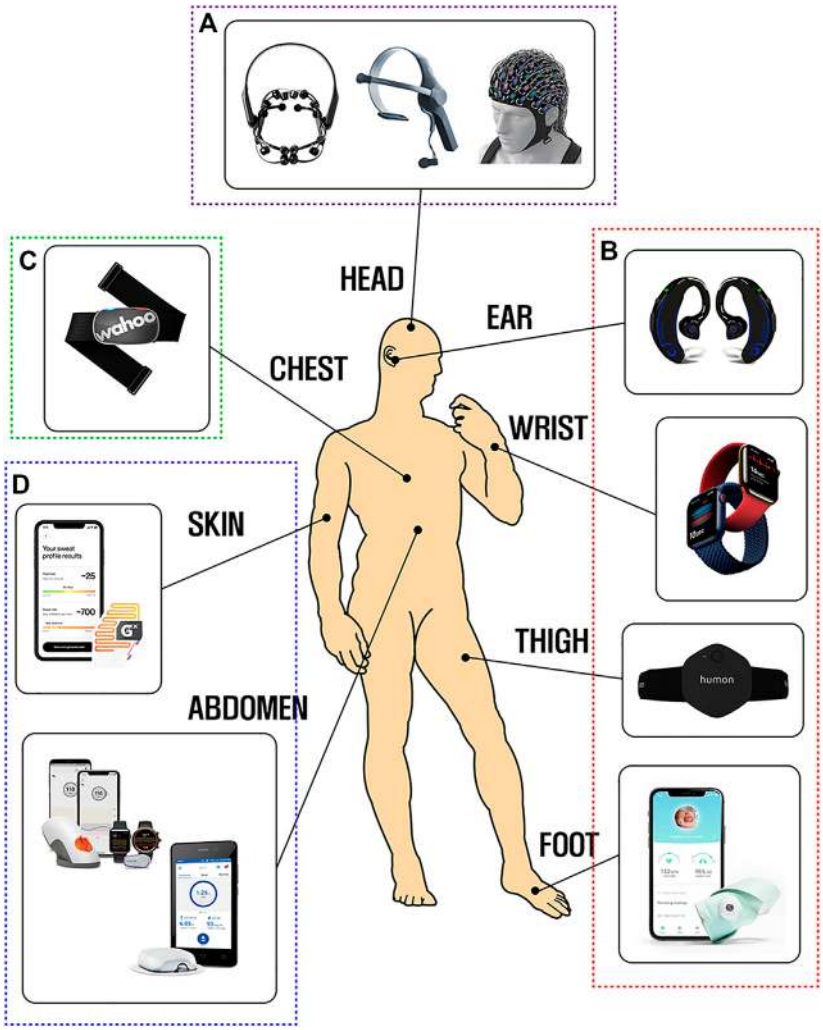

FIGURE 1 | State-of-the-art wearable healthcare devices: **(A)** EEG monitoring headset (EMOTIV, 2021; Cognionics, 2021; NeuroSky, 2021); **(B)** PPG devices in the form of earplug (FreeWavz, 2021), watch (Apple, 2021), band (Humon, 2021), and socks (Owlet, 2021); **(C)** heart rate monitoring device (Wahoo Fitness, 2021; and **(D)** skin contact sweat patch (Epicore Biosystems and Gatorade, 2021), continuous glucose monitoring system (Dexcom, 2021), and insulin management system (Insulet Corporation, 2021).

exercise, are also collected with wearable devices spread widely on the body in the form of smartwatch, earphone, clothes, and patch as depicted in **Figure 1B**. Moreover, the heart rate (HR) or biochemical levels (e.g., glucose) can be analyzed as well by using smartphone-linked wearable devices so as to help diagnose diseases such as arrhythmia or diabetes in daily life, as shown in **Figures 1C,D**.

As the demand for continuous monitoring bio-signals in daily life greatly increases, many attempts have been made to implement long-term robust recording of ambulatory bio-signals. Especially, wearable EEG and PPG devices are spotlighted owing to wide applications and prominent user convenience. EEG can provide long-term real-time neuromonitoring in a safe and noninvasive manner. Moreover, compared with other bio-signals, EEG has been used for the broader field of applications, including neurological disorder management, emotional monitoring, and brain–computer communication. In addition, PPG has received great attention in the wearable healthcare market because PPG enables single spot acquisition with convenient light-based devices, and therefore possibly allows for daily life cardiovascular monitoring for the management of major adult diseases. The significance of PPG recently skyrockets owing to its possibility for the early detection of COVID-19 (Guler et al., 2020).

However, unfortunately, the current wearable devices for EEG and PPG recording cannot completely avoid issues coming from motion artifacts. It is because motion artifacts typically are at least ten times greater in amplitude than bio-signals. Particularly, solving the artifact issues in EEG applications is a difficult task due to its smaller amplitude and nonstationary waveform than other bio-signals. For PPG monitoring, motion artifact caused by sensor displacement is a major signal distortion source in

ambulatory conditions. In addition to motion artifacts, many kinds of physiological artifacts and electromagnetic interference are also challenging hurdles of accurate EEG and PPG measurement in daily life.

While various articles rigorously review artifact reduction schemes for EEG (Xu et al., 2017; Jiang et al., 2019; Shad et al., 2020) and PPG (Periyasamy et al., 2017; Biswas et al., 2019), this article covers cross-border EEG motion artifact removal schemes that can be utilized at each part of the entire acquisition system: from the recording front-end hardware to the processing algorithm software, emphasizing the necessity of a diversified approach on the artifact issues. Furthermore, in-ear EEG researches that are actively studied in recent years are carefully reviewed from a perspective of the motion artifact removal. While a standard for classification of PPG motion artifact compensation methods based on the dependency relationship between motion artifact and PPG signals is suggested, techniques using learning-based systems such as deep learning and support vector machine are also included as emerging strategies.

In the following sections, we review state-of-the-art solutions tackling various motion artifacts in EEG and PPG wearable devices. In **Section 2**, the background of EEG and PPG including fundamentals, history, and research trends are studied. In **Section 3**, methods to alleviate motion artifact from EEG are reviewed in the aspects of the electrodes, electric circuits, and signal processing. In **Section 4**, PPG motion artifact compensation methods are presented with the relationship between PPG signal and motion artifact, followed by conclusion in **Section 5**.

2 FUNDAMENTALS OF BIO-SIGNALS

EEG and PPG are the most common bio-signals that are collected by wearable devices for research and/or clinical purposes. Therefore, in this section, the fundamentals of EEG and PPG are studied.

2.1 Electroencephalography (EEG)

Electroencephalography (EEG) is the brain's spontaneous electrical activity recorded on the scalp surface in a noninvasive fashion. It reflects the current flow during synchronized excitation of multiple pyramidal neurons in the cerebral cortex (Silva and da Silva, 2005; Teplan, 2002). International Federation's 10–20 system is used for standard electrode placement in human EEG recording (Jasper, 1958). The amplitude of scalp-recorded brain wave is approximately 20–200 μV and typically classified according to frequency: alpha (8–13 Hz), beta (14–30 Hz), gamma (> 30 Hz), theta (4–7 Hz), and delta (< 3.5 Hz) (Webster, 2009). EEG provides useful information on human brain functions including cognition (alertness and cognitive engagement), disease (epileptic seizure and sleep disorder), and the effect of drugs (Bickford, 1987).

Both applications and acquisition techniques of EEG have been significantly developed, as shown in **Figure 2A**. After Hans Berger (1873–1941) successfully obtained human EEG from the scalp, clinical EEG studies related especially on epilepsy were actively carried out by researchers including William G. Lennox (1884–1960) and Frederick Gibbs (1903–1999) (Mecarelli, 2019). Recently, the range of applications is being extended to sleep research, brain–computer interfaces (BCI), neuromarketing, neuroprosthesis, augmented cognition, and neurofeedback (Wolpaw et al., 2002; Xu and Zhong, 2018; Abiri et al., 2019). In addition to EEG applications, accurate and comfortable EEG acquisition techniques have been evolved by decreasing the size of EEG devices. Large EEG recording units should be located outside of recording sites. As such, a long wire connection between the recording unit and electrodes is mandatory. This results in various problems including motion artifact, limited mobility, cross-talk, and interference. However, recent small-form factor energy-efficient integrated circuit (IC) chips for an amplifier, an analog-to-digital converter (ADC), and a wireless transmitter allow for miniaturized battery-operated EEG units. Consequently, preparation process is much simplified, and long-term recording becomes more feasible (Casson et al., 2008).

As EEG technology has advanced, researchers attempted to record EEG from ear canals, called in-ear EEG (Looney et al., 2011; Kidmose et al., 2012). In order to assess the validity of in-ear EEG data, several well-known paradigms such as alpha attenuation response (AAR) and auditory steady-state response (ASSR) are widely utilized (Kidmose et al., 2013; Mikkelsen et al., 2015). These paradigms confirm that temporal lobe EEG and in-ear EEG contain similar information. Furthermore, the method to create an in-ear EEG forward model has been developed, which enables mapping the brain sources to potentials in the ear (Goverdovsky et al., 2017; Kappel et al., 2019a). In near future, the in-ear EEG method is expected to analyze EEG and treat brain diseases through both sound and electrical stimulation in real time by adding in-ear EEG recording function into a currently used wireless earphone.

2.2 Photoplethysmography (PPG)

Photoplethysmography (PPG) is a noninvasive photoelectric technique detecting blood volume changes in the microvascular bed of tissue (Challoner, 1979). The spectrum of PPG ranges from 0.5 to 4 Hz (Carr and Brown, 1998), while the amplitude of that heavily depends on transmitted power *via* a light source including a light-emitting device (LED). PPG signal is composed of slowly changing quasi-DC baseline and pulsatile components. Quasi-DC baseline is mostly induced by variation in reflection or transmission from the tissue, bone, and sympathetic nervous system, while pulsatile components are synchronous with the heartbeat (Utami et al., 2013). The signal is recorded by a pulse oximeter which computes peripheral oxygen saturation for clinical purposes using different light absorption rates on oxygenated hemoglobin (Sabeti et al., 2019). Heart rate monitoring based on PPG has become a popular alternative to that based on ECG since PPG signal can be recorded on a single spot of diverse body regions such as fingertips, wrists, or thighs (Castaneda et al., 2018). PPG also contains various vital information including cardiac output, arterial aging, endothelial function, and autonomic function (Allen, 2007).

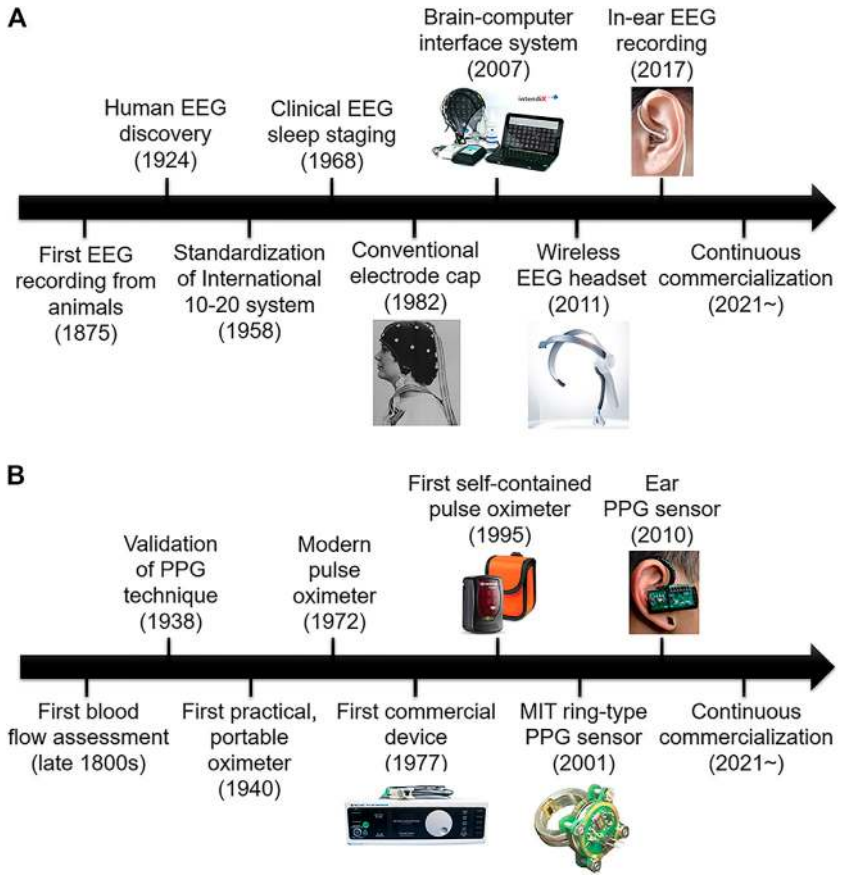

FIGURE 2 | History of bio-signals from its first experiment to modern commercialized products: **(A)** EEG (Blom and Anneveldt, 1982; g.tec, 2021; NeuroSky MindWave, 2021; Kappel, 2018) and **(B)** PPG (Nellcor, 2021; Nonin Medical, 2021; Tamura et al., 2014; Poh et al., 2010)

The development of the PPG technique from the first blood flow experiment to modern commercialized PPG products is shown in **Figure 2B** (Wolling et al., 2019). The first real-time blood flow assessment with early light bulbs was conducted in the late 1800s. From 1977, when the first commercial PPG device was successfully launched, the paradigm in commercialized PPG products has shifted from clinical use in medical industries to the use in the home environment with the development of a self-contained pulse oximeter. Also, the miniaturization allows for the usage of PPG devices as wearable devices. As a result, the PPG industry has been expanding beyond the existing nonambulatory applications such as sleep apnea detection toward ambulatory environments including personal monitoring devices in sports.

Especially, due to recent COVID-19, research interest in PPG devices dramatically increases. Under *silent hypoxia* which is an early stage of COVID-19, the oxygen saturation level of a patient decreases to a specific deficient level (less than 60%) without any symptom such as shortness of breath, leading to severe lung damage (Guler et al., 2020). However, since the PPG technique extracts oxygen saturation rate, a device continuously monitoring PPG possibly detects *silent hypoxia*.

3 ELECTROENCEPHALOGRAPHY MOTION ARTIFACT REMOVAL

EEG artifacts are undesirable inputs superimposed on measured EEG. Motions, electrophysiological signals excluding EEG, and electromagnetic interference, such as various sources, can cause artifacts. In both clinical and daily life applications, artifacts are a major hurdle in the interpretation of EEG signal since artifacts reduce the accuracy of automated classification of signal sequences for clinical diagnosis (Islam et al., 2020) and disturb the operation of the BCI system (Guarnieri et al., 2018). In particular, motion artifacts in wearable devices have been a key challenge due to the inevitable body and device movements.

3.1 Understanding of Electroencephalography Motion Artifact

Motion artifacts are unwanted electrical input induced by physical movements of the body and measurement system. There are two large categories of motion artifacts (Cao et al., 2015). First, motions of the measurement system physically disturb the signal path, which can be converted to motion

artifacts. Second, motions of subjects generate electrophysiological signals such as electromyogram (EMG) and electrooculogram (EOG), which is often superposed on EEG signals as artifacts. While the source of physiological artifacts is relatively clear, it needs to deeply study the main causes of motion artifact coming from the movement of the measurement system.

Figure 3 shows an electrical model of the EEG measurement system, which helps understanding the origin of motion artifacts. From the brain to the readout circuit, every body part and device component are composed of different materials transferring the brain signal from its source. Even distinguished parts are modeled as electrical components such as resistors and capacitors (Chi et al., 2010). A resistor R_{body} represents the resistance of brain tissues, cranium (skull), and inner layers of the skin. The electrical properties of inner tissues are simplified to a single resistor, R_{body}, since the resistance of the inner parts is relatively small and not controllable.

Electrode–skin interface (ESI) is physical contact of the outermost skin and the electrode. The impedance of ESI (Z_{ESI}) describes electrical characteristics between R_{body} and the impedance of the electrode, Z_E, and is strongly affected by the type of contact (wet, dry, and noncontact). The impedance of the outermost skin, called stratum corneum, is about $1M\Omega||10nF$ when the skin is dry. By applying the conductive gel or saline, the impedance value is reduced to $100k\Omega||10nF$, so wet electrodes minimize the signal attenuation (Shad et al., 2020). Other than the impedance of the stratum corneum, pressure, electrode structure, and skin environment factors such as sweat and hairs also influence the impedance of ESI since the ESI capacitance easily varies ranging from few pF to hundreds of pF by the contact status (Chi et al., 2010; Yousefi et al., 2020). This is the reason why dry and noncontact electrodes are much vulnerable to motion artifacts. Unfortunately, however, for wearable device applications, dry and noncontact electrodes are preferable over wet electrodes owing to the possibility of their long-term use and user convenience. Motions of the measurement system swing the ESI impedance and result in distortion and disturbance in EEG recording. The voltage gain from V_{signal} to V_{in} is

$$V_{in} = \frac{Z_{in.Amp.}}{Z_{path} + Z_{in.Amp.}} V_{signal}, \tag{1}$$

where $Z_{path} = R_{Body} + Z_{ESI} + Z_E$. This formula emphasizes the impact of Z_{ESI} variation, which directly changes the amplitude of the output signal due to gain distortion (Song et al., 2014; Dabbaghian et al., 2019).

In addition to the gain variation, the change of ESI capacitance generates the unwanted current across the ESI, expressed in

$$i_C(t) = C\frac{dV_C}{dt} + V_C\frac{dC}{dt}, \tag{2}$$

where C, V_C, and i_C are the ESI capacitance, the voltage across the C, and the current flow through the C, respectively. If the ESI capacitance changes while a voltage across the capacitor is applied, the charges stored in the capacitance flow in order to compensate for the capacitance change. Since the input impedance of the readout circuits is high, the current is converted into voltage and appears in the EEG signal as drifting baseline (Mihajlović et al., 2013; Yousefi et al., 2020).

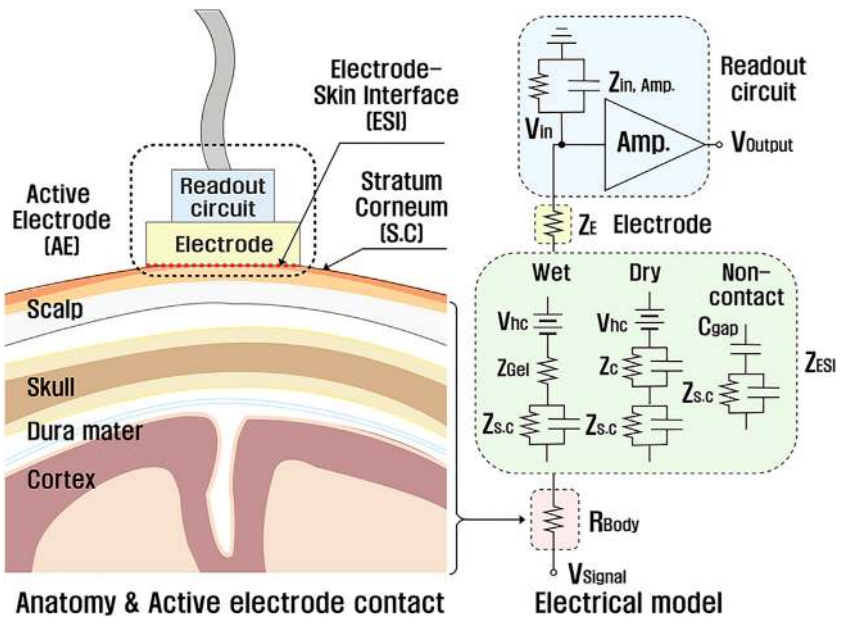

FIGURE 3 | An anatomical graphic of the EEG signal path and the corresponding electrical model (Chi et al., 2010; Shad et al., 2020). V_{signal}: voltage signal from the brain; V_{in}: readout circuit input signal; Z_{ESI}, Z_{gel}, $V_{s.c}$, and Z_E: impedance values of ESI, conductive gel, stratum corneum, and electrode, respectively; $Z_{in.Amp}$: input impedance of the readout circuit; V_{hc}: half-cell potential; Z_c: contact impedance at ESI; C_{gap}: capacitance at the noncontact interface.

Half-cell potential fluctuation is also a significant source of motion artifacts. **Figure 4** visualizes the electrical model of the ESI with a pair of electrodes (wet or dry) collecting a differential input. Even using two identical electrodes, half-cell potentials may be different from each other, and the difference of half-cell potentials slowly varies possibly due to movement. This is a main culprit for large time-varying DC offset (wet electrodes: $< 50mV$, dry electrodes: $< 300mV$) (Liu et al., 2020). Moreover, the impedance mismatch between two ESIs induced from movements reduces the common-mode rejection ratio (CMRR) of the differential recording. This is a significant issue since the common-mode signal ($(V_{signal1} + V_{signal2})/2$) is typically two or three orders of magnitude larger than differential signal $(V_{signal1} - V_{signal2})/2$.

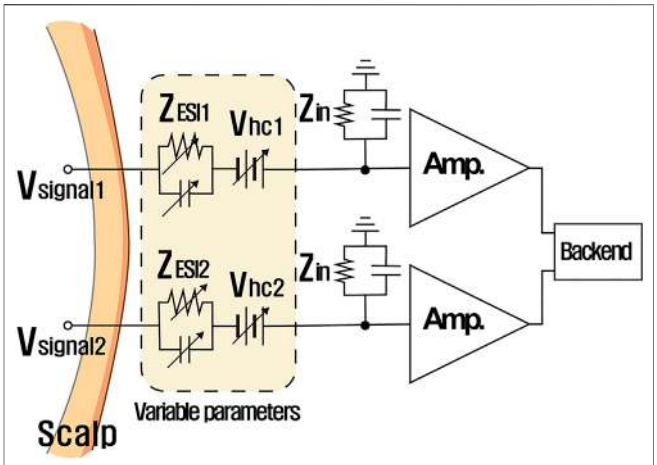

FIGURE 4 | Electrical model of the ESI and two electrodes: variability of the ESI impedance and the half-cell potential causes motion artifacts.

3.2 Methods to Reduce Electroencephalography Motion Artifacts

For wearable applications, methods to alleviate motion artifacts are especially important compared to clinical EEG applications focusing on blocking electromagnetic interference and other physiological signals such as ECG and EOG (McFarland et al., 1997; Fatourechi et al., 2007). There is no single omnipotent solution to solve all motion artifact issues. Various methods applied to each part of the EEG recording system including electrodes, readout circuits, and digital processing should be studied altogether (Fatourechi et al., 2007).

3.2.1 Types of Electrodes

Shapes and materials of electrodes determine impedance and stability of the ESI. Wet Ag/AgCl electrodes (**Figure 5A**) are common in clinical EEG recording owing to its high stability, low ESI impedance ($\ll 100k\Omega$), and thus, low noise level (Li et al., 2017). Dry electrodes (**Figure 5B**) have been utilized in wearable EEG devices for better user convenience (Matsuo et al., 1973; Taheri et al., 1994; Grozea et al., 2011). The ESI impedance of dry electrode for one square centimeter is about $1M\Omega$ at 10 Hz (Chen et al., 2014), which is much bigger than that of wet electrodes. While noncontact electrode possibly removes half-cell potential variation, it could induce a significant baseline drifting.

Considering the stability of ESI and motion artifacts, dry contact electrodes have been regarded as a gold standard for long-term EEG wearable devices. As such, various shapes and materials of dry electrodes have been suggested. Fingers of dry electrodes were designed to avoid incomplete and unstable contacts caused by hairs at the ESI (**Figure 5C**). To prevent the movements at the contact interface and improve user comfort, dry electrodes made of flexible materials (**Figure 5D**), such as ethylene propylene diene monomer (EPDM) and polydimethyl-siloxane (PDMS), were developed. Some dry flexible electrodes modified from finger types show better performance. Reverse-curve arch-shaped dry electrode (**Figure 5E**) and bristle-type electrode (**Figure 5F**) have a larger contact area and thus smaller ESI impedance, and the flexibility of the material provides better user comfort. Furthermore, to overcome the high impedance of dry electrodes, microneedle array electrodes (MAE) were developed. Microneedles penetrate the stratum corneum ($15 - 20\,\mu m$) and reduce the ESI impedance to the wet electrode level ($\ll 100k\Omega$) (**Figure 5G**) (Ren et al., 2020a, Ren et al., 2020b).

On the other hand, another type called semidry electrodes (**Figure 5H**) supply a minimal amount of conductive fluid/gel on the interface by continuously supplying the liquid from its reservoir. A semidry electrode maintains the interface to have conductive fluid of tens of microliter (Li et al., 2020) so that the amount of fluid is less than that of a wet electrode ($1 - 2mL$). For this reason, the ESI impedance of semidry electrodes is about tens of $k\Omega$ at 1kHz, and the short-term and the long-term stability are comparable to those of wet electrodes (Li et al., 2017).

The structure and the physical properties of entire EEG recording systems are also important for interface contact. When the stable contact is supported by applying mechanical pressure using springs, motion artifact occurrence is relatively avoided (Chen et al., 2015). A flexible, thin, and light EEG-recording system implemented with a flexible printed circuit board (FPCB) and small IC technologies (**Figure 5I**) provides tight contact to the forehead.

3.2.2 Active Electrode and Analog Circuits

Recent advances in IC technologies enable a bench-top recording system to become wearable by locating integrated small-form factor amplifiers directly on the electrodes. This architecture is called active electrode (AE) and removes long wire connection between electrodes and a recording system (Xu et al., 2017). By minimizing the wire connection, this active electrode architecture has various advantages over passive electrodes: 1) it shortens high impedance connection which is very vulnerable to any interference, 2) it allows the recording system to have ultrahigh input impedance ($\sim T\Omega$), 3) it minimizes motion artifacts induced from wire tension, and 4) it enables wireless wearable devices. To further reduce motion artifact effects, AEs may contain additional circuitry to enhance input impedance, eliminate DC offsets, and reduce the effect of ESI variation.

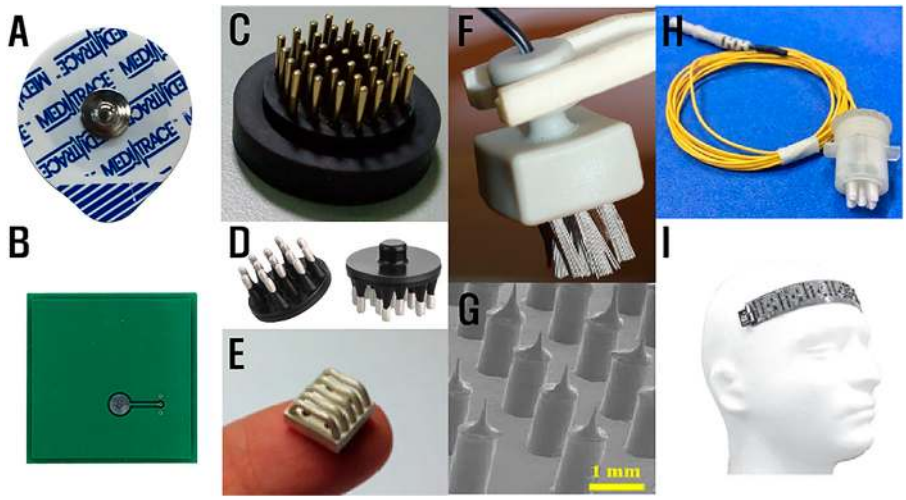

FIGURE 5 | Types of electrodes: **(A)** patch-type wet electrode, **(B)** dry electrode, **(C)** dry electrode with fingers (Liao et al., 2009), **(D)** flexible dry electrode (Dätwyler, 2021), **(E)** reverse-curve arch-shaped dry electrode (Lee et al., 2015), **(F)** bristle-type electrode (Grozea et al., 2011), **(G)** microneedle electrode (Ren et al., 2020a)), **(H)** semi-wet electrode (Wang et al., 2016), and **(I)** flexible EEG system (Dabbaghian et al., 2019).

Impedance bootstrapping is a popular method to boost the input impedance of AEs. The current supplied by a positive feedback loop, I_{fb}, cancels the input current from an electrode I_{in} to charge Z_{in}, as illustrated in **Figure 6A**. When I_{fb} is equal to I_{ib}, input impedance seen from the electrode becomes infinite (Xu et al., 2017). However, it is not easy to exactly estimate Z_{in}. Furthermore, the loop gain of the positive feedback should be less than unity for stability. Therefore, fine-tuning of Z_{fb} is necessary. Several works achieve high input impedance ranging from hundreds of $M\Omega$ to few $T\Omega$ (Chi et al., 2011; Xu et al., 2011). Other methods increasing the input impedance have also been suggested. The nullification of MOSFET parasitic capacitance by a unity-gain buffer and active shielding of the input signal line successfully minimizes the parasitic capacitance (Joshi et al., 2016). In addition, in chopper-stabilized amplifiers, input coupling capacitors are regularly switched, and pre-charging of the input coupling capacitors by buffers before the chopping phase also decreases the input capacitance (Chandrakumar and Marković, 2016).

For the compensation of DC offset induced by the half-cell potential variation by movement, an integrator is often inserted in a negative feedback loop of the instrumentation amplifier, and this loop is called a DC servo loop (DSL) (**Figure 6B**) (Song et al., 2015). DSL sets the output DC voltage as a reference level *via* negative feedback, regardless of the input DC level. It removes frequency components below the integrator cutoff frequency that is usually near 0.1 Hz. To attain low cutoff frequency, a $G\Omega$ range resistance is required. In CMOS applications, resistor-emulating

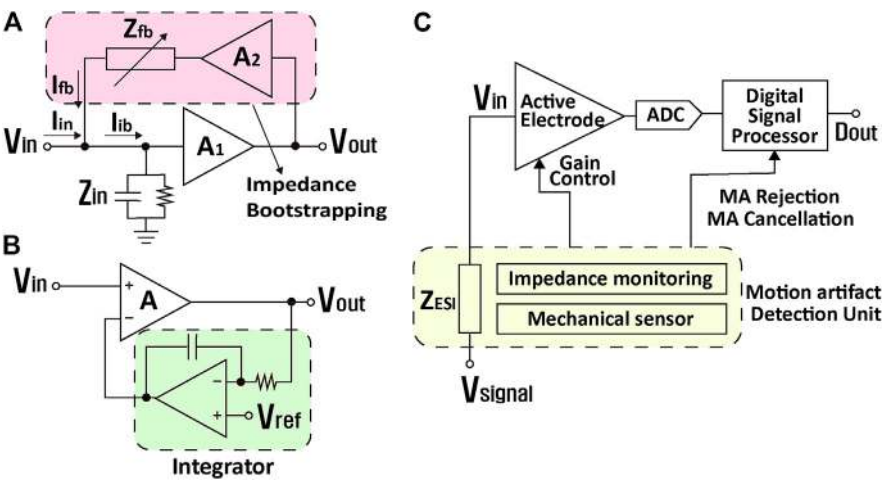

FIGURE 6 | Various circuit techniques in active electrode architectures for motion artifact reduction. **(A)** Input impedance boosting, **(B)** DC offsets elimination, and **(C)** motion artifact detection.

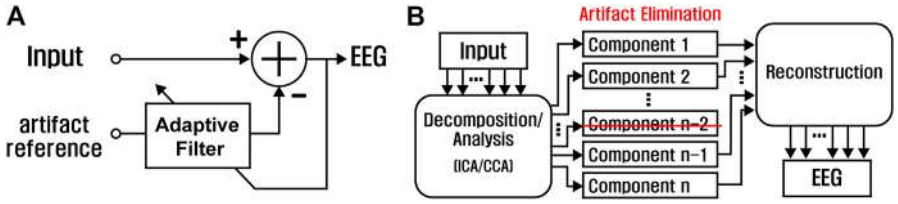

FIGURE 7 | Signal processing schemes for EEG motion artifact removal: **(A)** adaptive filter and **(B)** blind-source separation.

circuits such as pseudo-resistors, switched-capacitor resistors, and switched-resistor resistors are adopted (Xu et al., 2017). Since the time constant of the integrator is large, an active electrode with the DSL often takes a long time for DC settlement. Digitally controlled DC servo loop (DCDSL) can relieve this issue by supplying instant large current when V_{out} is outside a certain range (Schönle et al., 2013; Liu et al., 2020).

Figure 6C shows a technique that monitors the ESI variation induced from movement and compensates for the effect of the variation by controlling the gain of an amplifier, deleting recorded data, or separating clean EEG signal from contaminated data. For the ESI monitoring, an additional sensor is required that monitors the ESI impedance. This impedance sensor 1) injects current to the ESI and measures voltage at the ESI (Bertrand et al., 2013; Song et al., 2014), or 2) applies intentional DC bias to the ESI and measures amplified current induced by movement based on **Eq. 2** (Dabbaghian and Kassiri, 2020). In addition, movement itself can be directly detected by using a mechanical sensor (Goverdovsky et al., 2014; Nordin et al., 2018). Based on the sensed information, contaminated EEG data by motion are either recovered by separating/offsetting motion artifact only, or ignored by not transferring them to D_{out}.

3.2.3 Signal Processing Algorithms

Signal processing algorithms are powerful for EEG artifact removal. Various processing methods including regression, adaptive filtering, blind-source separation (BSS), single-channel source separation, and machine learning have been applied. For proper application of each method, the types of targeted artifacts, the number of signal channels, and the existence of artifact-referencing channels should be considered. In many cases, two or more methods are used together to obtain the optimum efficacy.

Regression subtracts artifacts from contaminated EEG signals under an assumption that the measured EEG is the linear combination of clean EEG and artifacts. The artifacts can be estimated from artifact-referencing electrodes or raw contaminated EEG signals. For EOG and ECG artifacts whose origins are relatively clear, artifact-referencing electrodes provide information on the artifacts (Fortgens and De Bruin, 1983; Woestenburg et al., 1983). Adaptive filter (**Figure 7A**) is a concept extended from regression, in which the weight for the artifact subtraction is continuously modified by filter algorithms such as least mean squares (LMS) (Marque et al., 2005).

Recent removal methods tend to avoid using any artifact-referencing electrode or other prior information. Blind-source separation (BSS) is a group of algorithms for separating artifact components from multiple-channel EEG signals (**Figure 7B**), such as independent component analysis (ICA) and canonical correlation analysis (CCA) (Jiang et al., 2019). ICA finds a set of signal components by decomposing multichannel EEG so that each component has maximum non-Gaussianity. Artifact components are manually or automatically selected among the separated components and then removed, resulting in clean EEG (Albera et al., 2012; Oliveira et al., 2016). CCA utilizes the correlations among the dataset. Using the fact that EEG typically has high autocorrelation coefficients while EMG has low coefficients, CCA is able to effectively remove EMG artifacts (Radüntz et al., 2017; Chen et al., 2018). Other physiological artifacts having low autocorrelation coefficients are also possibly removed by CCA.

Moreover, source separation techniques for single-channel EEG based on wavelet transform (WT) and empirical mode decomposition (EMD) are also frequently used. Wavelet transform decomposes a signal into a sum of wavelet functions, with coefficients encoding both time and frequency domain information. Threshold method or total variation denoising scheme filters out artifact components to restore the clean EEG signal (Krishnaveni et al., 2007; Gajbhiye et al., 2019). EMD is an algorithm to decompose a nonlinear and nonstationary signal into a certain set of intrinsic mode functions (IMF). EMD is used by itself or together with other source separation methods such as ICA, CCA, and WT to remove physiological artifacts and motion artifacts (Safieddine et al., 2012; Bono et al., 2016; Chen et al., 2018). Furthermore, machine learning algorithms such as supervised learning are combined with the source separation techniques for detecting and classifying artifacts automatically (Jafari et al., 2017; Radüntz et al., 2017).

3.3 Methods to Reduce In-Ear Electroencephalography Motion Artifacts

Even though EEG measurement technology has made great progress on human brain monitoring, conventional EEG devices have several drawbacks in using it in daily life, including large volume, weight, and long preparation time. Therefore, these EEG devices have been mostly used for clinical and research purposes only. To tackle these difficulties,

recent research trend is guided to implementing comfortable EEG devices. One of the great examples is an in-ear EEG device, which records EEG from within the ear canal using embedded electrodes on an earplug-shaped earpiece (Looney et al., 2011; Kidmose et al., 2012), as shown in **Figure 8**.

There are some crucial advantages of in-ear EEG compared to conventional EEG. First, earpieces are compact, unobtrusive, and comfortable, enabling devices to become more portable and wearable for everyday use (Looney et al., 2012; Kidmose et al., 2013). Second, electrodes on earpieces are held firmly in place owing to the tight fit between the earpiece and the ear canal, resulting in fewer motion artifacts (Looney et al., 2012). Third, any electromagnetic interference is significantly reduced because conductive medium such as skin and tissue surrounds the ear canal (Looney et al., 2011). Last, EEG recording modules including artifact reduction schemes can be integrated in a commonly used Bluetooth earphone, opening a window toward a healthcare earphone in near future. By these structural and electrical advantages, in-ear EEG is gaining significant research interests. Especially, earpiece, electrode, and circuit design to measure more accurate EEG signals as well as to reduce motion artifacts are studied.

Early studies have mostly used customized earpieces which fix electrodes in certain ear canal position tightly, minimizing the effect of user movement (Kidmose et al., 2013; Bleichner et al., 2015; Mikkelsen et al., 2015). Generic reusable earpieces, however, are indispensable for commercializing the in-ear EEG system that all users can use immediately in real life. Several kinds of generic earpieces are developed by using memory foam with Ag-coated cloth (Goverdovsky et al., 2016, Goverdovsky et al., 2017; Nakamura et al., 2018), Ag spray-coated polycarbonate (Kaveh et al., 2020), CNT/PDMS-based canal-type ear electrode cap (CEE) (Lee et al., 2014), and silvered glass silicone CEE (Dong et al., 2016). Viscoelastic flexibility and pressure between earpiece materials and ear canal allow a device to be held more softly and firmly, reducing both motion artifacts and user discomfort.

In addition to changing materials of earpieces and electrodes, circuit design techniques also significantly reduce motion artifacts. Although in-ear EEG is more immune to eye blinking, it is yet vulnerable to artifacts caused by jaw and head movement because of its passive electrode with long wire connection (Kappel et al., 2014; Kappel et al., 2017). Following on-scalp EEG, dry and active electrode circuits using impedance boosting, DC servo loop, and active shielding techniques are also applied to the in-ear EEG system for motion artifact reduction (Zhou et al., 2016; Kappel and Kidmose, 2018; Kappel et al., 2019b; Lee et al., 2019). All of these circuit architectures can be implemented by recent advanced integrated circuit (IC) technology for miniaturization. Furthermore, measuring in-ear EEG using wireless communication technology such as Bluetooth low energy (BLE) is utilized to diminish the effects of wire connections (Dong et al., 2016; Lee et al., 2019; Kaveh et al., 2020). Therefore, it is possible to minimize the size of the device and to transfer recorded EEG data to the mobile phones wirelessly, enabling further reduction of motion artifacts. **Table 1** shows a comparison of the state-of-the-art in-ear EEG studies.

4 PHOTOPLETHYSMOGRAPHY MOTION ARTIFACT REMOVAL

PPG is also vulnerable to various artifacts. Here, factors of artifacts and compensation techniques depending on the statistical relationship between PPG and motion artifacts are presented.

4.1 Understanding of Photoplethysmography Motion Artifact

A complete PPG signal can be simply modeled with the following representations (Shaltis, 2008):

$$Input = N_{amb.} + N_{mech.} + N_{elec.} + N_{vas.} + S_{vas.}, \quad (3)$$

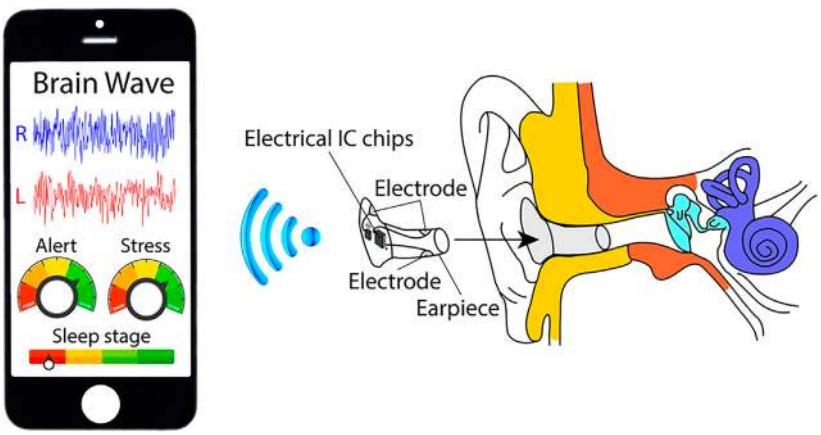

FIGURE 8 | Wireless in-ear EEG recording concept (Looney et al., 2012).

TABLE 1 | Comparison between recent in-ear EEG studies.

References	Electrode material	Contact type	Channel/ earpiece	Electrode area (mm^2)	Wireless	Earpiece style	Artifact rejection
Kidmose et al. (2012)	Ag	Wet	2	20	N	Custom	—
Lee et al. (2014)	CNT/PDMS	Dry	1	—	N	Generic	Standard–shaped Flexible earpiece
Goverdovsky et al. (2016)	Ag-coated Nylon cloth	Wet	2	40	N	Generic	Viscoelastic memory foam earpiece
Zhou et al. (2016)	—	Dry	2	0.8*	N	Custom	Active electrode, DSL, impedance boosting
Dong et al. (2016)	Silvered glass silicon	Dry	1	—	Y*	Generic	Electrode with soft supporting material
Kappel et al. (2019b)	IrO_2	Dry	6**	9.6	N	Custom	Active shielding Flexible joint earpiece
Lee et al. (2019)	—	Dry	2	—	Y	Custom	Wireless EEG Recording IC chip
Kaveh et al. (2020)	Ag	Dry	4	60	Y	Generic	Wireless neural Recording module

*Estimated.
**All electrodes on earpiece.

where *Input* is a total PPG signal, while $N_{amb.}$, $N_{mech.}$, $N_{elec.}$, $N_{vas.}$, and $S_{vas.}$ are the effects of environmental light, movement of PPG sensors on skins, electrical noise from sensors, vascular dynamics by physiological phenomena, and the signal of interest created by blood pulsation, respectively. **Eq. 3** can be simplified by excluding $N_{amb.}$ and $N_{elec.}$ with an assumption that these factors can be minimized by proper circuit techniques such as chopping stabilization and low-noise circuit design techniques. $N_{mech.}$ and $N_{vas.}$ are related to motion, and thus, the sum of these two factors can be considered as motion artifacts, as illustrated in **Figure 9**. Motion artifact is a major hindrance in high-quality recording of PPG signal (Poets and Stebbens, 1997; Hayes and Smith, 1999; Rhee et al., 2001).

4.2 Methods to Reduce Photoplethysmography Motion Artifacts

Conventional spectrum filtering methods have limitations on compensating for motion artifacts since the spectrum of body motions and that of PPG signal are partially overlapped (Rusch et al., 1996). Therefore, methods have been developed to solve the problem, depending on sources of PPG signal and motion artifact.

4.2.1 Independence-Based Compensation

If the event of motion has no or limited impact on blood pulsation, then PPG and motion artifacts are considered as independent. Several compensation methods under the assumption of the independence between PPG and motion artifacts have been suggested. Among them, three important techniques such as independent component analysis (ICA), adaptive noise cancellation (ANC), and Fourier series analysis (FSA) are studied.

One of the most representative source separation techniques for independent variables is ICA, as shown in **Figure 10A**. The purpose of the algorithm is to estimate unmixing matrix W to separate n independent sources from m mixtures where mixtures are assumed to follow Gaussian distribution, and usually, $m = n$ (Hyvarinen, 1999). To draw non-Gaussian sources from the mixtures, an initial W is set at first. It is multiplied with the mixture matrix (M), and the joint probability distribution function of $W \times M$ is obtained. Likelihood function $l(W, M)$ of the distribution function is estimated and partially differentiated by W. Then, W is updated until $l(W, M)$ gets the extreme point where the Gaussianity of the joint probability distribution function is minimized. Finally, independent m sources are obtained through $S = W \times M$. To increase the

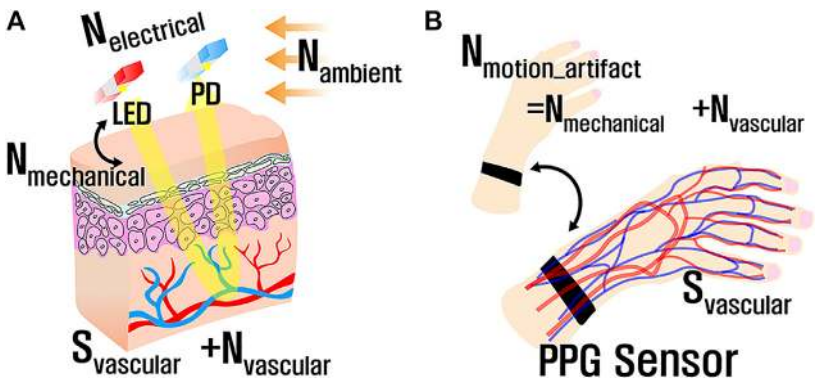

FIGURE 9 | Major factors for PPG recording: **(A)** environmental and vascular factors for PPG recording and **(B)** simplified model focusing on motion artifacts.

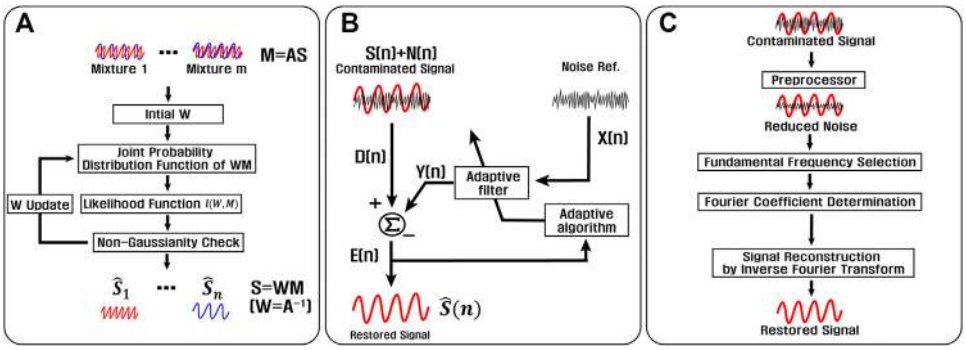

FIGURE 10 | Motion artifact reduction techniques applicable for independent sources: **(A)** schematic of the independent component analysis (ICA) method, **(B)** schematic of the adaptive noise cancellation method (ANC), and **(C)** schematic of the Fourier series analysis method.

performance of the ICA algorithm and to overcome information loss, pre- and/or post-processors are used (Kim and Yoo, 2006; Krishnan et al., 2010; Ram et al., 2013; Lo and Meng, 2016; Luke et al., 2018). As an example of preprocessing, ICA-based improved dual-tree complex wavelet transform (I^2DTCWT) (Ram et al., 2013) separates cardiac component first and applies ICA algorithm to obtain motion artifact without losing the respiratory information. Finally, by subtracting motion artifacts from contaminated input, PPG signal with intact respiratory data can be restored.

Figure 10B shows an adaptive noise cancellation (ANC) scheme that is very useful when noise references are available (Liang et al., 2015). For motion artifact reduction, noise references reflect various motion information (Chowdhury et al., 2018; Arunkumar and Bhaskar, 2020). By applying an adaptive filter to input from noise references, $Y(n)$ is obtained. $Y(n)$ should be as close to that of the original noise component $N(n)$ as possible. This is conducted by iterative processes changing the weight coefficient of the adaptive filter. The difference output $E(n)$ finally becomes the estimated clean PPG signal $\widehat{S}(n)$ when the gradient of power of $E(n)$ crosses a zero point from negative to positive in iterative processes. Owing to its simple algorithm, the speed of the ANC algorithm is fast. The algorithm, however, is vulnerable when $S(n)$ and $N(n)$ are spectrally overlapped (Zhang et al., 2015; Yang et al., 2018).

Fourier series analysis (FSA) illustrated in **Figure 10C** (Bracewell, 2000) is based on the Fourier theorem that any periodic signal can be decomposed into a set of sinusoidal waveforms including a fundamental frequency and its harmonics. A contaminated PPG signal is first trimmed by a preprocessor such as a bandpass filter to decrease noise. Then, the fundamental frequency of PPG is determined by period-detection algorithms, and Fourier coefficients of the fundamental and representative harmonics are calculated (Yang and Tang, 2014; Sadhukhan et al., 2018). By applying inverse Fourier transform to these coefficients, a clean PPG signal is reconstructed. In addition, techniques for FSA are further improved (Reddy et al., 2009; Raj et al., 2019). For example, the fundamental frequency is obtained by cycle-by-cycle Fourier series analysis (CFSA) for a short time window to overcome the quasiperiodicity of PPG.

4.2.2 Dependence-Based Compensation

Whether PPG and motion artifact are independent or not is an ongoing controversial issue (Reddy and Kumar, 2007; Ram et al., 2012; Agarwal et al., 2013; Raghuram et al., 2014; Nie et al., 2020). The possibility that motion can affect arterial flow has been increased (Yao and Warren, 2005; Lo et al., 2017). The arterial volume variation in a stationary condition $\overrightarrow{dA_s}$ and that in a motion condition $\overrightarrow{dA_m}$ were carefully studied, which insists that the correlation between $\overrightarrow{dA_s}$ and $\overrightarrow{dA_m}$ is less than a half for every event of motion. This means that motion might affect arterial volume variation, and thus subsequently PPG signals. Therefore, software-based techniques compensating dependent motion artifacts have been actively developed. The algorithms are mainly divided into two categories without/with learning-based artificial intelligence systems, which is illustrated in **Figure 11**.

For motion artifact reduction methods without learning-based systems, analyses on time domain (**Figure 11A**) and frequency domain (**Figure 11B**) are regarded. A signal-subtraction method with two PPG channels is used for the time-based analysis (Lee et al., 2016). Two PPG channels have different light intensities, and thus PPG signals and motion artifacts obtained from the two channels are different, respectively. More importantly, the power ratio between two PPG signals and that between motion artifacts are also different since brighter light decreases the effect of motion artifact (Branche and Mendelson, 2005). First, the two channels with different light intensity measure PPG signals in stable condition, and a gain of one channel is adjusted until the difference of the PPG powers becomes zero. Then, in the case of corrupted PPG signals, the gain is multiplied to the one channel such that PPG signals from two channels become identical, and the subtraction process follows. As a result, only motion artifact with reduced amplitude remains. This remaining motion artifact is calibrated to recover a clean

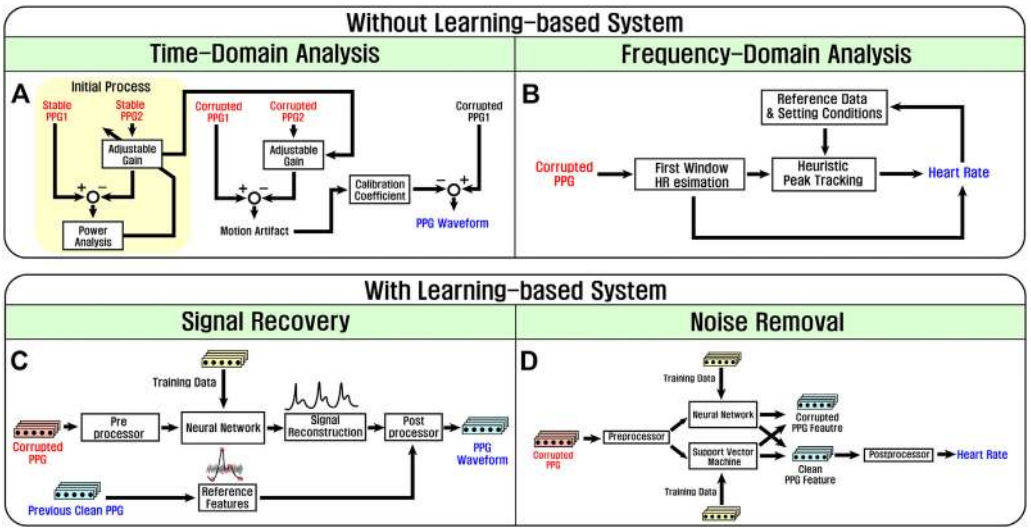

FIGURE 11 | Overview of motion artifact compensation techniques regarding dependence relationship between PPG and motion artifact signals. **(A)** Time domain compensation method, **(B)** frequency domain compensation method, **(C)** noise recovery which restores PPG waveform with the neural network system, **(D)** noise removal which sorts out contaminated PPG with the neural network system and support vector machine.

PPG signal. In addition, a heuristic method in the frequency domain is applied which estimates HR values for series of time windows on the frequency domain with the assumption that HR is not abruptly changed. HR of each time window is determined based on the spectrum peaks of the window and the previous HR value (Zhu et al., 2015).

On the other hand, learning-based compensation methods are mainly classified into two categories by the output forms: clean PPG waveform and HR. A signal recovery method shown in **Figure 11C** uses artificial neural network (ANN) trained by PPG features such as pulse width, pulse interval, and systolic amplitude. To get a clean PPG signal, a contaminated PPG signal is preprocessed such as bandpass filtering and baseline drift removal. Furthermore, reference features of the PPG signal are saved for post-processing. Inputs are processed by trained ANN and dived to reconstruction process such as an interpolation-based restoration algorithm (Ghosal et al., 2020). Then, postprocessor such as glitch noise removal or calibration using stored reference features is implemented to enhance the quality of outputs. Moreover, a signal reconstruction is sometimes conducted inside learning-based systems. For example, a signal–noise interaction modeling-based algorithm for motion artifact removal (SniMA) utilizes a time-delay neural network (TDNN) to generate a noise-free PPG vector using the information of PPG and motion artifact at different timestamps (Xu et al., 2020).

The learning-based noise removal technique cuts out contaminated parts of PPG using classification processes as shown in **Figure 11D**. The feature extraction of PPG signals is pre-conducted and qualified to train the systems such as ANN and support vector machine (SVM). ANN generally shows better classification accuracy when training data are given enough, while SVM achieves better classification performance when data are not sufficient (Longjie and Abeysekera, 2019; Liu S. H. et al., 2020). Various types of training data are used to obtain clean PPG features (Chang et al., 2019; Liu X. et al., 2020). For example, interpolated PPG data estimated from ECG by the DeepHeart algorithm and contaminated PPG are provided to train convolution neural network (CNN) for enhancing classification performance. Finally, corrupted and clean PPG features are separated by

TABLE 2 | Comparison between recent PPG studies.

References	Target MA	Compasation type	Target output	Compensation method	Else devices	Learning based
Raghuram et al. (2014)	IDP[a]	Recovery	Waveform	I^2DTCWT	—	N
Reddy et al. (2009)	IDP	Recovery	Waveform	CFSA	—	N
Roy et al. (2018)	IDP	Recovery	Waveform	PCA/ANN	—	Y
Zhu et al. (2015)	IDP/DP[b]	Removal	HR	MICROST	Accelerometer	N
Chang et al. (2019)	IDP/DP	Removal	HR	Deepheart	—	Y
Xu et al. (2020)	IDP/DP	Recovery	Waveform	SniMA	Accelerometer/gyroscope	Y

[a]*Indepdenent.*
[b]*Dependent.*

trained ANN or SVM. Representative PPG compensation methods are organized in **Table 2**.

5 CONCLUSION

This article reviews motion artifact removal techniques for wearable EEG and PPG sensor systems with the basic understandings of EEG and PPG technology and the origins of motion artifacts. For EEG devices, diverse approaches are applicable at each part of the acquisition system. Electrodes, analog readout circuits, and additional signal processing units are studied and recently applied to solve the EEG motion artifact issues. In addition, earpiece materials and ASICs have been developed for motion artifact removal in in-ear EEG. For PPG motion artifact removal, several compensation methods such as independent component analysis, adaptive noise cancellation, and techniques without/with learning-based algorithms are presented. The majority of modern artifact reduction methods have adopted independence-based analysis, while the number of dependence-based analyses is gradually increased. Artifact reduction techniques are continuously being developed to cover both independent and dependent motion artifacts.

Recent trends of wearable EEG and PPG device development are miniaturization by improving energy efficiency for battery size reduction. It is because miniaturization is one of the key factors toward motion artifact reduction. Along with the development of semiconductor and material engineering, in the near future, the size of bio-signal sensors will further decrease, and complex software-oriented processes along with analog signal recording/stimulation are possibly developed on a single chip. Furthermore, learning-based methods will be consistently enhanced and be a great solution for challenging motion artifact issues with the help of artificial intelligence.

AUTHOR CONTRIBUTIONS

Paper conception and design, and drafting of manuscript: DS, SL, MK, and CK; EEG motion artifact removal: DS, MK, and CK; PPG motion artifact removal: SL and CK; final editing of manuscript: DS, SL, MK, JC, and CK.

FUNDING

This work has been supported by the National Research Foundation of Korea (NRF) grant funded by the Korea government (MSIT) (nos. 2019R1G1A110059411 and 2020R1C1C1009878) and been supported by the Technology Innovation Program (no. 20012464) funded by the Ministry of Trade, Industry and Energy (MOTIE, Korea).

REFERENCES

Abiri, R., Borhani, S., Sellers, E. W., Jiang, Y., and Zhao, X. (2019). A Comprehensive Review of EEG-Based Brain-Computer Interface Paradigms. *J. Neural Eng.* 16, 011001. doi:10.1088/1741-2552/aaf12e

Agarwal, A., Singh, A., Acharyya, A., Shafik, R. A., and Ahamed, S. R. (2013). "Energy-Efficient and High-Speed Robust Channel Identification Methodology to Solve Permutation Indeterminacy in ICA for Artifacts Removal from ECG in Remote Healthcare," in 2013 International Symposium on Electronic System Design, December 10–12, 2013. 52–56. doi:10.1109/ISED.2013.17

Albera, L., Kachenoura, A., Comon, P., Karfoul, A., Wendling, F., Senhadji, L., et al. (2012). ICA-based EEG Denoising: a Comparative Analysis of Fifteen Methods. *Bull. Polish Acad. Sci. Tech. Sci.* 60, 407–418. doi:10.2478/v10175-012-0052-3

Allen, J. (2007). Photoplethysmography and its Application in Clinical Physiological Measurement. *Physiol. Measurementm IOP Sci.* 28. doi:10.1088/0967-3334/28/3/R01

Apple (2021). Apple (Watch Series 6). Available at: https://www.apple.com/kr/apple-watch-series-6/.

Arunkumar, K. R., and Bhaskar, M. (2020). Robust De-noising Technique for Accurate Heart Rate Estimation Using Wrist-type PPG Signals. *IEEE Sensors J.* 20, 7980–7987. doi:10.1109/JSEN.2020.2982540

Aun, N. F. M., Soh, P. J., Al-Hadi, A. A., Jamlos, M. F., Vandenbosch, G. A. E., and Schreurs, D. (2017). Revolutionizing Wearables for 5G: 5G Technologies: Recent Developments and Future Perspectives for Wearable Devices and Antennas. *IEEE Microwave Mag.* 18, 108–124. doi:10.1109/MMM.2017.2664019

Silva, F. H., and da Silva, F. L. (2005). *Electroencephalography: Basic Principles, Clinical Applications, and Related Fields*. Pennsylvania, PA: Lippincott Williams & Wilkins.

Beniczky, S., Karoly, P., Nurse, E., Ryvlin, P., and Cook, M. (2020). Machine Learning and Wearable Devices of the Future. *Epilepsia n/a.* 62, S116–S124. doi:10.1111/epi.16555

Bertrand, A., Mihajlović, V., Grundlehner, B., Van Hoof, C., and Moonen, M. (2013). "Motion Artifact Reduction in EEG Recordings Using Multi-Channel Contact Impedance Measurements," in 2013 IEEE Biomedical Circuits and Systems Conference (BioCAS), Cleveland, OH, October 31–November 2, 2013, 258–261. doi:10.1109/BioCAS.2013.667968

Bickford, R. D. (1987). "Electroencephalography," in *Encyclopedia of Neuroscience*. Editors G. Adelman (Cambridge, United Kingdom: Birkhäuser). doi:10.2514/6.1987-1943

Biswas, D., Simões-Capela, N., Van Hoof, C., and Van Helleputte, N. (2019). Heart Rate Estimation from Wrist-Worn Photoplethysmography: A Review. *IEEE Sensors J.* 19, 6560–6570. doi:10.1109/JSEN.2019.2914166

Bleichner, M. G., Lundbeck, M., Selisky, M., Minow, F., Jäger, M., Emkes, R., et al. (2015). Exploring Miniaturized EEG Electrodes for Brain-Computer Interfaces. An EEG You Do Not See? *Physiol. Rep.* 3, e12362. doi:10.14814/phy2.12362

Blom, J., and Anneveldt, M. (1982). An Electrode Cap Tested. *Electroencephalog. Clin. Neurophysiol.* 54, 591–594. doi:10.1016/0013-4694(82)90046-3

Bono, V., Das, S., Jamal, W., and Maharatna, K. (2016). Hybrid Wavelet and EMD/ICA Approach for Artifact Suppression in Pervasive EEG. *J. Neurosci. Method.* 267, 89–107. doi:10.1016/j.jneumeth.2016.04.006

Bracewell, R. N. (2000). *The Fourier Transform and its Applications*. 3rd ed. New York, NY: McGraw-Hill.

Branche, P., and Mendelson, Y. (2005). "Signal Quality and Power Consumption of a New Prototype Reflectance Pulse Oximeter Sensor," in Proceedings of the IEEE 31st Annual Northeast Bioengineering Conference, 2005, Hoboken, NJ, April 2–3, 2005. 42–43. doi:10.1109/NEBC.2005.1431917

Cao, K., Guo, Y., and Su, S. W. (2015). "A Review of Motion Related EEG Artifact Removal Techniques," in 2015 9th International Conference on Sensing Technology (ICST), Auckland, New Zealand, December 8–10, 2015, 600–604. doi:10.1109/ICSensT.2015.7438469

Carr, J. J., and Brown, J. M. (1998). *Introduction to Biomedical Equipment Technology*. Upper Saddle River, NJ: Prentice-Hall.

Casson, A. J., Smith, S., Duncan, J. S., and Rodriguez-Villegas, E. (2008). "Wearable EEG: what Is it, Why Is it Needed and what Does it Entail?," in 2008 30th Annual International Conference of the IEEE Engineering in Medicine and

Biology Society, Vancouver, BC, Augest 20–24, 2008, 5867–5870. doi:10.1109/IEMBS.2008.4650549

Castaneda, D., Esparza, A., Ghamari, M., Soltanpur, C., and Nazeran, H. (2018). A Review on Wearable Photoplethysmography Sensors and Their Potential Future Applications in Health Care. *Int. J. Biosens. Bioelectron.* 4, 195–202. doi:10.15406/ijbsbe.2018.04.00125

Challoner, A. V. J. (1979). *Photoelectric Plethysmography for Estimating Cutaneous Blood Flow*. London, United Kingdom: Academic Press.

Chamola, V., Hassija, V., Gupta, V., and Guizani, M. (2020). A Comprehensive Review of the COVID-19 Pandemic and the Role of IoT, Drones, AI, Blockchain, and 5G in Managing its Impact. *IEEE Access* 8, 90225–90265. doi:10.1109/ACCESS.2020.2992341

Chandrakumar, H., and Marković, D. (2016). "5.5 A 2μW 40mVpp Linear-Input-Range Chopper- Stabilized Bio-Signal Amplifier with Boosted Input Impedance of 300MΩ and Electrode-Offset Filtering," in 2016 IEEE International Solid-State Circuits Conference (ISSCC), San Francisco, CA, January 31–February 4, 2016, 96–97. doi:10.1109/ISSCC.2016.7417924

Chang, X., Li, G., Tu, L., Xing, G., and Hao, T. (2019). "DeepHeart: Accurate Heart Rate Estimation from PPG Signals Based on Deep Learning," in 2019 IEEE 16th International Conference on Mobile Ad Hoc and Sensor Systems (MASS), Monterey, CA, November 4–7, 2019, 371–379. doi:10.1109/MASS.2019.00051

Chen, Y.-H., De Beeck, M., Vanderheyden, L., Carrette, E., Mihajlović, V., Vanstreels, K., et al. (2014). Soft, Comfortable Polymer Dry Electrodes for High Quality ECG and EEG Recording. *Sensors* 14, 23758–23780. doi:10.3390/s141223758

Chen, Y.-C., Lin, B.-S., and Pan, J.-S. (2015). Novel Noncontact Dry Electrode with Adaptive Mechanical Design for Measuring EEG in a Hairy Site. *IEEE Trans. Instrumentation Meas.* 64, 3361–3368. doi:10.1109/tim.2015.2459531

Chen, X., Xu, X., Liu, A., McKeown, M. J., and Wang, Z. J. (2018). The Use of Multivariate EMD and CCA for Denoising Muscle Artifacts from Few-Channel EEG Recordings. *IEEE Trans. Instrumentation Meas.* 67, 359–370. doi:10.1109/tim.2017.2759398

Chi, Y. M., Jung, T.-P., and Cauwenberghs, G. (2010). Dry-Contact and Noncontact Biopotential Electrodes: Methodological Review. *IEEE Rev. Biomed. Eng.* 3, 106–119. doi:10.1109/rbme.2010.2084078

Chi, Y. M., Maier, C., and Cauwenberghs, G. (2011). Ultra-High Input Impedance, Low Noise Integrated Amplifier for Noncontact Biopotential Sensing. *IEEE J. Emerging Selected Top. Circuits Syst.* 1, 526–535. doi:10.1109/jetcas.2011.2179419

Chowdhury, S. S., Hyder, R., Hafiz, M. S. B., and Haque, M. A. (2018). Real-Time Robust Heart Rate Estimation from Wrist-type PPG Signals Using Multiple Reference Adaptive Noise Cancellation. *IEEE J. Biomed. Health Inform.* 22, 450–459. doi:10.1109/JBHI.2016.2632201

Cognionics (2021). Cognionics (Mobile-128). Available at: https://www.cgxsystems.com/mobile-128.

Dabbaghian, A., and Kassiri, H. (2020). "An 8-Channel 0.45mm2/Channel EEG Recording IC with ADC-free Mixed-Signal In-Channel Motion Artifact Detection and Removal," in 2020 IEEE International Symposium on Circuits and Systems (ISCAS), Sevilla, Spain, May 17–20, 2020. 1–5. doi:10.1109/ISCAS45731.2020.9181024

Dabbaghian, A., Yousefi, T., Fatmi, S. Z., Shafia, P., and Kassiri, H. (2019). A 9.2-g Fully-Flexible Wireless Ambulatory EEG Monitoring and Diagnostics Headband with Analog Motion Artifact Detection and Compensation. *IEEE Trans. Biomed. Circuits Syst.* 13, 1141–1151. doi:10.1109/tbcas.2019.2936327

Dätwyler (2021). Dätwyler (SoftPulse™). Available at: https://datwyler.com/healthcare-solutions/healthcare/wearables-digital-health/softpulse.

Dexcom (2021). Dexcom (G6). Available at: https://www.dexcom.com/ko-KR.

Dias, D., and Paulo Silva Cunha, J. (2018). Wearable Health Devices—Vital Sign Monitoring, Systems and Technologies. *Sensors* 18. doi:10.3390/s18082414

Dong, H., Matthews, P. M., and Guo, Y. (2016). "A New Soft Material Based In-The-Ear EEG Recording Technique," in 2016 38th Annual International Conference of the IEEE Engineering in Medicine and Biology Society, Orlando, FL, August 16–20, 2016 (New York, NY, United States: EMBC). 5709–5712. doi:10.1109/EMBC.2016.7592023

Emotiv (2021). Emotiv (Epoc-X.). Available at: https://www.emotiv.com/epoc-x/.

Epicore Biosystems and Gatorade (2021). Epicore Biosystems and Gatorade (Gx Sweat Patch). Available at: https://www.gatorade.com/gx/gx-sweat-patch/.

Fatourechi, M., Bashashati, A., Ward, R. K., and Birch, G. E. (2007). EMG and EOG Artifacts in Brain Computer Interface Systems: A Survey. *Clin. Neurophysiol.* 118, 480–494. doi:10.1016/j.clinph.2006.10.019

Fortgens, C., and De Bruin, M. P. (1983). Removal of Eye Movement and ECG Artifacts from the Non-cephalic Reference EEG. *Electroencephalography Clin. Neurophysiol.* 56, 90–96. doi:10.1016/0013-4694(83)90010-x

FreeWavz (2021). FreeWavz (Smart Earphones). Available at: http://www.freewavz.com/store/freewavz-blue/.

g.tec (2021). g.tec (intendiX). Available at: https://www.gtec.at/history/and https://singularityhub.com/2010/03/07/intendix-the-brain-computer-interface-goes-commercial-video/.

Gajbhiye, P., Tripathy, R. K., Bhattacharyya, A., and Pachori, R. B. (2019). Novel Approaches for the Removal of Motion Artifact from EEG Recordings. *IEEE Sensors J.* 19, 10600–10608. doi:10.1109/JSEN.2019.2931727

Ghosal, P., Himavathi, S., and Srinivasan, E. (2020). "PPG Motion Artifact Reduction Using Neural Network and Spline Interpolation," in 2020 7th International Conference on Smart Structures and Systems (ICSSS), Chennai, India, July 23–24, 2020, 1–6. doi:10.1109/ICSSS49621.2020.9202214

Goverdovsky, V., Looney, D., Kidmose, P., and Mandic, D. P. (2014). "Multimodal Physiological Sensor for Motion Artefact Rejection," in 2014 36th Annual International Conference of the IEEE Engineering in Medicine and Biology Society, Chicago, Illinois, August 26–30, 2014 (IEEE), 2753–2756. doi:10.1109/embc.2014.6944193

Goverdovsky, V., Looney, D., Kidmose, P., and Mandic, D. P. (2016). In-Ear EEG from Viscoelastic Generic Earpieces: Robust and Unobtrusive 24/7 Monitoring. *IEEE Sensors J.* 16, 271–277. doi:10.1109/JSEN.2015.2471183

Goverdovsky, V., von Rosenberg, W., Nakamura, T., Looney, D., Sharp, D. J., Papavassiliou, C., et al. (2017). Hearables: Multimodal Physiological In-Ear Sensing. *Scientific Rep.* 7. doi:10.1038/s41598-017-06925-2

Grozea, C., Voinescu, C. D., and Fazli, S. (2011). Bristle-sensors–low-cost Flexible Passive Dry EEG Electrodes for Neurofeedback and BCI Applications. *J. Neural Eng.* 8, 025008. doi:10.1088/1741-2560/8/2/025008

Guarnieri, R., Marino, M., Barban, F., Ganzetti, M., and Mantini, D. (2018). Online EEG Artifact Removal for BCI Applications by Adaptive Spatial Filtering. *J. Neural Eng.* 15, 056009. doi:10.1088/1741-2552/aacfdf

Guler, U., Costanzo, I., and Sen, D. (2020). Emerging Blood Gas Monitors: How They Can Help with COVID-19. *IEEE Solid-State Circuits Mag.* 12, 33–47. doi:10.1109/MSSC.2020.3021839

Hayes, M. J., and Smith, P. R. (1999). "Quantitative Evaluation of Photoplethysmographic Artifact Reduction for Pulse Oximetry," in *Biomedical Sensors, Fibers, and Optical Delivery Systems*. Editors. F. Baldini, N. I. Croitoru, M. Frenz, I. Lundstroem, M. Miyagi, R. Pratesi, et al. (Bellingham, WA, United States: International Society for Optics and Photonics (SPIE)), Vol. 3570, 138–147. doi:10.1117/12.336924

Hedayatipour, A., and Mcfarlane, N. (2020). Wearables for the Next Pandemic. *IEEE Access* 8, 184457–184474. doi:10.1109/ACCESS.2020.3029130

Humon (2021). Humon (Hex Muscle Oxygen Sensor). Available at: https://humon.io/.

Hyvarinen, A. (1999). Fast and Robust Fixed-point Algorithms for Independent Component Analysis. *IEEE Trans. Neural Network.* 10, 626–634. doi:10.1109/72.761722

Insulet Corporation (2021). Insulet Corporation (Omnipod DASH). Available at: https://www.omnipod.com/new-to-omnipod.

Islam, M. S., El-Hajj, A. M., Alawieh, H., Dawy, Z., Abbas, N., and El-Imad, J. (2020). EEG Mobility Artifact Removal for Ambulatory Epileptic Seizure Prediction Applications. *Biomed. Signal Process. Control.* 55, 101638. doi:10.1016/j.bspc.2019.101638

Jafari, A., Gandhi, S., Konuru, S. H., David Hairston, W., Oates, T., and Mohsenin, T. (2017). "An EEG Artifact Identification Embedded System Using ICA and Multi-Instance Learning," in 2017 IEEE International Symposium on Circuits and Systems (ISCAS), Baltimore, MD, May 28–31, 2017. 1–4. doi:10.1109/ISCAS.2017.8050346

Jasper, H. H. (1958). The Ten-Twenty Electrode System of the International Federation. *Electroencephalography Clin. Neurophysiol.* 10, 371–375. doi:10.1016/0013-4694(58)90053-1

Jiang, X., Bian, G.-B., and Tian, Z. (2019). Removal of Artifacts from EEG Signals: A Review. *Sensors* 19, 987. doi:10.3390/s19050987

Joshi, S., Kim, C., and Cauwenberghs, G. (2016). A 6.5- μ*W*/MHz Charge Buffer with 7-fF Input Capacitance in 65-nm CMOS for Noncontact Electropotential Sensing. *IEEE Trans. Circuits Syst. Express Briefs* 63, 1161–1165. doi:10.1109/tcsii.2016.2623591

Kappel, S. L., and Kidmose, P. (2018). "Real-Life Dry-Contact Ear-EEG," in 2018 40th Annual International Conference of the IEEE Engineering in Medicine and Biology Society, Honolulu, HI, July 18–21, 2018 (New York, NY, United States: EMBC). 5470–5474. doi:10.1109/EMBC.2018.8513532

Kappel, S. L., Looney, D., Mandic, D. P., and Kidmose, P. (2014). "A Method for Quantitative Assessment of Artifacts in EEG, and an Empirical Study of Artifacts," in 2014 36th Annual International Conference of the IEEE Engineering in Medicine and Biology Society, Chicago, Illinois. August 26–30, 204, 1686–1690. doi:10.1109/EMBC.2014.6943931

Kappel, S. L., Looney, D., Mandic, D. P., and Kidmose, P. (2017). Physiological Artifacts in Scalp EEG and Ear-EEG. *BioMedical Eng. OnLine* 16. doi:10.1186/s12938-017-0391-2

Kappel, S. L., Makeig, S., and Kidmose, P. (2019a). Ear-EEG Forward Models: Improved Head-Models for Ear-EEG. *Front. Neurosci.* 13, 943. doi:10.3389/fnins.2019.00943

Kappel, S. L., Rank, M. L., Toft, H. O., Andersen, M., and Kidmose, P. (2019b). Dry-Contact Electrode Ear-EEG. *IEEE Trans. Biomed. Eng.* 66, 150–158. doi:10.1109/TBME.2018.2835778

Kappel, S. L. (2018). *Development and Characterization of Ear-EEG for Real-Life Brain-Monitoring*. Aarhus, Denmark: AU Library Scholarly Publishing Services. doi:10.7146/aul.260.183

Kaveh, R., Doong, J., Zhou, A., Schwendeman, C., Gopalan, K., Burghardt, F. L., et al. (2020). Wireless User-Generic Ear EEG. *IEEE Trans. Biomed. Circuits Syst.* 14, 727–737. doi:10.1109/TBCAS.2020.3001265

Kidmose, P., Looney, D., and Mandic, D. P. (2012). "Auditory Evoked Responses from Ear-EEG Recordings," in 2012 Annual International Conference of the IEEE Engineering in Medicine and Biology Society, San Diego, CA, August 28–Septembet 1, 2012, 586–589. doi:10.1109/EMBC.2012.6345999

Kidmose, P., Looney, D., Ungstrup, M., Rank, M. L., and Mandic, D. P. (2013). A Study of Evoked Potentials from Ear-EEG. *IEEE Trans. Biomed. Eng.* 60, 2824–2830. doi:10.1109/TBME.2013.2264956

Kim, B. S., and Yoo, S. K. (2006). Motion Artifact Reduction in Photoplethysmography Using Independent Component Analysis. *IEEE Trans. Biomed. Eng.* 53, 566–568. doi:10.1109/TBME.2005.869784

Krishnan, R., Natarajan, B., and Warren, S. (2010). Two-Stage Approach for Detection and Reduction of Motion Artifacts in Photoplethysmographic Data. *IEEE Trans. Biomed. Eng.* 57, 1867–1876. doi:10.1109/TBME.2009.2039568

Krishnaveni, V., Jayaraman, S., Anitha, L., and Kalidoss, R. (2007). Removal of Ocular Artifacts from EEG Using Adaptive Thresholding of Wavelet Coefficients. *J. Neural Eng.* 3, 338–346. doi:10.1088/1741-2560/3/4/011

Lee, J. H., Lee, S. M., Byeon, H. J., Hong, J. S., Park, K. S., and Lee, S.-H. (2014). CNT/PDMS-based Canal-Typed Ear Electrodes for Inconspicuous EEG Recording. *J. Neural Eng.* 11, 046014. doi:10.1088/1741-2560/11/4/046014

Lee, J. S., Han, C. M., Kim, J. H., and Park, K. S. (2015). Reverse-curve-arch-shaped Dry EEG Electrode for Increased Skin-Electrode Contact Area on Hairy Scalps. *Electro. Lett.* 51, 1643–1645. doi:10.1049/el.2015.1873

Lee, H., Ko, H., Thap, T., and Lee, J. (2016). "Multiple Switching Light Sources Based Motion Artifacts Reduction in Reflectance Photoplethysmography," in 2016 38th Annual International Conference of the IEEE Engineering in Medicine and Biology Society, Orlando, FL, August 16–20, 2016 (New York, NY, United States: EMBC), 3398–3401. doi:10.1109/EMBC.2016.7591457

Lee, J., Lee, K., Ha, U., Kim, J., Lee, K., Gweon, S., et al. (2019). A 0.8-V 82.9- μ W In-Ear BCI Controller IC with 8.8 PEF EEG Instrumentation Amplifier and Wireless BAN Transceiver. *IEEE J. Solid-State Circuits* 54, 1185–1195. doi:10.1109/JSSC.2018.2888845

Li, G., Wang, S., and Duan, Y. Y. (2017). Towards Gel-free Electrodes: A Systematic Study of Electrode-Skin Impedance. *Sensors Actuators B: Chem.* 241, 1244–1255. doi:10.1016/j.snb.2016.10.005

Li, G.-L., Wu, J.-T., Xia, Y.-H., He, Q.-G., and Jin, H.-G. (2020). Review of Semi-dry Electrodes for EEG Recording. *J. Neural Eng.* 17, 051004. doi:10.1088/1741-2552/abbd50

Liang, B., Iwnicki, S., Ball, A., and Young, A. (2015). Adaptive Noise Cancelling and Time-Frequency Techniques for Rail Surface Defect Detection. *Mech. Syst. Signal Process.* 54–55, 41–51. doi:10.1016/j.ymssp.2014.06.012

Liao, L., Chao, P. C., Chen, Y., Lin, C., Ko, L., Lin, H., et al. (2009). A Novel Hybrid Bioelectrode Module for the Zero-Prep EEG Measurements. *Sensors*, 939–942. doi:10.1109/ICSENS.2009.5398180

LifeSignals (2021). LifeSignals (Biosensor Patch). Available at: https://lifesignals.com/covid19/.

Liu, L., Hua, T., Zhang, Y., Mu, J., and Zhu, Z. (2020). A Robust Bio-IA with Digitally Controlled DC-Servo Loop and Improved Pseudo-resistor. *IEEE Trans. Circuits Syst. Express Briefs* 67, 440–444. doi:10.1109/tcsii.2019.2922423

Liu, S. H., Liu, H. C., Chen, W., and Tan, T. H. (2020a). Evaluating Quality of Photoplethymographic Signal on Wearable Forehead Pulse Oximeter with Supervised Classification Approaches. *IEEE Access* 8, 185121–185135. doi:10.1109/ACCESS.2020.3029842

Liu, X., Hu, Q., Yuan, H., and Yang, C. (2020b). "Motion Artifact Detection in PPG Signals Based on Gramian Angular Field and 2-D-CNN," in 2020 13th International Congress on Image and Signal Processing, BioMedical Engineering and Informatics, Chengdu, China, October 17–19, 2020 (CISP-BMEI). 743–747. doi:10.1109/CISP-BMEI51763.2020.9263630

Lo, F. P., and Meng, M. Q. (2016). "Double Sensor Complementary Placement Method to Reduce Motion Artifacts in PPG Using Fast Independent Component Analysis," in 2016 38th Annual International Conference of the IEEE Engineering in Medicine and Biology Society, Orlando, FL, August 16–20, 2016 (New York, NY, United States: EMBC), 3179–3182. doi:10.1109/EMBC.2016.7591404

Lo, F. P., Li, C. X., Wang, J., and Meng, M. Q. (2017). "Motion Artifact Reduction in Photoplethysmogram Signals Based on Periodic Component Factorization," in 2017 39th Annual International Conference of the IEEE Engineering in Medicine and Biology Society, Jeju Island, Korea, July 15–16, 2017 (New York, NY, United States: EMBC), 1812–1815. doi:10.1109/EMBC.2017.8037197

Longjie, L., and Abeysekera, S. S. (2019). "Motion Artefact Removal Using Single Beat Classification of Photoplethysmographic Signals," in 2019 IEEE International Symposium on Circuits and Systems (ISCAS), Hokkaido, Japan, May 26–29, 2019, 1–4. doi:10.1109/ISCAS.2019.8702180

Looney, D., Park, C., Kidmose, P., Rank, M. L., Ungstrup, M., Rosenkranz, K., et al. (2011). "An In-The-Ear Platform for Recording Electroencephalogram," in 2011 Annual International Conference of the IEEE Engineering in Medicine and Biology Society, Québec, Canada, July 20–24, 2011, 6882–6885. doi:10.1109/IEMBS.2011.6091733

Looney, D., Kidmose, P., Park, C., Ungstrup, M., Rank, M. L., Rosenkranz, K., et al. (2012). The In-The-Ear Recording Concept: User-Centered and Wearable Brain Monitoring. *IEEE Pulse* 3, 32–42. doi:10.1109/MPUL.2012.2216717

Luke, A., Shaji, S., and Unnikrishna Menon, K. A. (2018). "Motion Artifact Removal and Feature Extraction from PPG Signals Using Efficient Signal Processing Algorithms," in 2018 International Conference on Advances in Computing, Communications and Informatics (ICACCI), Bangalore, India, September 19–22, 2018, 624–630. doi:10.1109/ICACCI.2018.8554599

Marque, C., Bisch, C., Dantas, R., Elayoubi, S., Brosse, V., and Pérot, C. (2005). Adaptive Filtering for ECG Rejection from Surface EMG Recordings. *J. Electromyogr. Kinesiol.* 15, 310–315. doi:10.1016/j.jelekin.2004.10.001

Matsuo, T., Iinuma, K., and Esashi, M. (1973). A Barium-Titanate-Ceramics Capacitive-type EEG Electrode. *IEEE Trans. Biomed. Eng. BME* 20, 299–300. doi:10.1109/tbme.1973.324197

McFarland, D. J., McCane, L. M., David, S. V., and Wolpaw, J. R. (1997). Spatial Filter Selection for EEG-Based Communication. *Electroencephalography Clin. Neurophysiol.* 103, 386–394. doi:10.1016/s0013-4694(97)00022-2

Mecarelli, O. (2019). *Clinical Electroencephalography*. New York NY: Springer International Publishing.

Mihajlović, V., Li, H., Grundlehner, B., Penders, J., and Schouten, A. C. (2013). "Investigating the Impact of Force and Movements on Impedance Magnitude and Eeg," in 2013 35th Annual International Conference of the IEEE Engineering in Medicine and Biology Society, Osaka, Japan, July 3–7, 2013 (New York, NY, United States: EMBC), 1466–1469. doi:10.1109/EMBC.2013.6609788

Mikkelsen, K. B., Kappel, S. L., Mandic, D. P., and Kidmose, P. (2015). EEG Recorded from the Ear: Characterizing the Ear-EEG Method. *Front. Neurosci.* 9, 438. doi:10.3389/fnins.2015.00438

Nakamura, T., Alqurashi, Y. D., Morrell, M. J., and Mandic, D. P. (2018). "Automatic Detection of Drowsiness Using In-Ear EEG," in 2018

International Joint Conference on Neural Networks (IJCNN), Rio de Janeiro, Brazil, July 08–13, 2018, 1–6. doi:10.1109/IJCNN.2018.8489723

Nellcor (2021). Nellcor (N-100). Available at: https://www.drstoystore.com/product/nellcor-n-100-pulse-oximeter/.

NeuroSky (2021). NeuroSky (MindWave Mobile 2). Available at: https://store.neurosky.com/pages/mindwave.

NeuroSky MindWave (2021). NeuroSky (MindWave). Available at: https://www.realwire.com/releases/NeuroSky-Breaks-Guinness-World-Record-to-launch-the-Mindwave-headset.

Nie, L., Berckmans, D., Wang, C., and Li, B. (2020). Is Continuous Heart Rate Monitoring of Livestock a Dream or Is it Realistic? A Review. *Sensors* 20. doi:10.3390/s20082291

Nonin Medical (2021). Nonin Medical (Onyx Vantage 9590). Available at: https://www.nonin.com/products/9590/ and https://www.hopkinsmedicalproducts.com/pulse-oximeters/p/Onyx-Vantage-9590-Pulse-Oximeter/.

Nordin, A. D., Hairston, W. D., and Ferris, D. P. (2018). Dual-electrode Motion Artifact Cancellation for Mobile Electroencephalography. *J. Neural Eng.* 15, 056024. doi:10.1088/1741-2552/aad7d7

Oliveira, A. S., Schlink, B. R., Hairston, W. D., König, P., and Ferris, D. P. (2016). Induction and Separation of Motion Artifacts in EEG Data Using a Mobile Phantom Head Device. *J. Neural Eng.* 13, 036014. doi:10.1088/1741-2560/13/3/036014

Owlet (2021). Owlet (Smart Sock 3). Available at: https://owletcare.com/products/owlet-smart-sock.

Periyasamy, V., Pramanik, M., and Ghosh, P. (2017). Review on Heart-Rate Estimation from Photoplethysmography and Accelerometer Signals during Physical Exercise. *J. Indian Inst. Sci.* 97. doi:10.1007/s41745-017-0037-1

Poets, C., and Stebbens, V. (1997). Detection of Movement Artifact in Recorded Pulse Oximeter Saturation. *Eur. J. Pediatr.* 156, 808–811. doi:10.1007/s004310050719

Poh, M., Swenson, N. C., and Picard, R. W. (2010). Motion-tolerant Magnetic Earring Sensor and Wireless Earpiece for Wearable Photoplethysmography. *IEEE Trans. Inf. Technol. Biomed.* 14, 786–794. doi:10.1109/TITB.2010.2042607

Radüntz, T., Scouten, J., Hochmuth, O., and Meffert, B. (2017). Automated EEG Artifact Elimination by Applying Machine Learning Algorithms to ICA-Based Features. *J. Neural Eng.* 14, 046004. doi:10.1088/1741-2552/aa69d1

Raghuram, M., Sivani, K., and Reddy, K. A. (2014). "E2MD for Reduction of Motion Artifacts from Photoplethysmographic Signals," in 2014 International Conference on Electronics and Communication Systems (ICECS), Coimbatore, India, February 13–14, 2014, 1–6. doi:10.1109/ECS.2014.6892793

Raj, R., Selvakumar, J., and Maik, V. (2019). AFODSS: Heart Rate Estimation Method from Photoplethysmographic Signals with Motion Artifacts Using Fourier-Sparse Dual Optimization. *IEEE Sensors J.* 19, 9953–9963. doi:10.1109/JSEN.2019.2928643

Ram, M. R., Madhav, K. V., Krishna, E. H., Komalla, N. R., and Reddy, K. A. (2012). A Novel Approach for Motion Artifact Reduction in PPG Signals Based on AS-LMS Adaptive Filter. *IEEE Trans. Instrumentation Meas.* 61, 1445–1457. doi:10.1109/TIM.2011.2175832

Ram, M. R., Madhav, K. V., Krishna, E. H., Komalla, N. R., Sivani, K., and Reddy, K. A. (2013). ICA-based Improved DTCWT Technique for MA Reduction in PPG Signals with Restored Respiratory Information. *IEEE Trans. Instrumentation Meas.* 62, 2639–2651. doi:10.1109/TIM.2013.2259114

Reddy, K. A., and Kumar, V. J. (2007). "Motion Artifact Reduction in Photoplethysmographic Signals Using Singular Value Decomposition," in 2007 IEEE Instrumentation Measurement Technology Conference IMTC 2007, Warsaw, Poland, May 1–3, 2007, 1–4. doi:10.1109/IMTC.2007.379467

Reddy, K. A., George, B., and Kumar, V. J. (2009). Use of Fourier Series Analysis for Motion Artifact Reduction and Data Compression of Photoplethysmographic Signals. *IEEE Trans. Instrumentation Meas.* 58, 1706–1711. doi:10.1109/TIM.2008.2009136

Ren, L., Chen, Z., Wang, H., Dou, Z., Liu, B., and Jiang, L. (2020a). Fabrication of Bendable Microneedle-Array Electrode by Magnetorheological Drawing Lithography for Electroencephalogram Recording. *IEEE Trans. Instrumentation Meas.* 69, 8328–8334. doi:10.1109/tim.2020.2990523

Ren, L., Liu, B., Zhou, W., and Jiang, L. (2020b). A Mini Review of Microneedle Array Electrode for Bio-Signal Recording: A Review. *IEEE Sensors J.* 20, 577–590. doi:10.1109/jsen.2019.2944847

Rhee, Sokwoo., Yang, Boo-Ho., and Asada, H. H. (2001). Artifact-resistant Power-Efficient Design of Finger-Ring Plethysmographic Sensors. *IEEE Trans. Biomed. Eng.* 48, 795–805. doi:10.1109/10.930904

Roy, S. M., Gupta, R., Chandra, J. K., Das Sharma, K., and Talukdar, A. (2018). Improving Photoplethysmographic Measurements Under Motion Artifacts Using Artificial Neural Network for Personal Healthcare. *IEEE Transactions on Instrumentation and Measurement* 67 (12), 2820–2829. doi:10.1109/TIM.2018.2829488

Rusch, T., Sankar, R., and Scharf, J. (1996). Signal Processing Methods for Pulse Oximetry. *Comput. Biol. Med.* 26, 143–159. doi:10.1016/0010-4825(95)00049-6

Sabeti, E., Reamaroon, N., Mathis, M., Gryak, J., Sjoding, M., and Najarian, K. (2019). Signal Quality Measure for Pulsatile Physiological Signals Using Morphological Features: Applications in Reliability Measure for Pulse Oximetry. *Inform. Med. Unlocked* 16, 100222. doi:10.1016/j.imu.2019.100222

Sadhukhan, D., Pal, S., and Mitra, M. (2018). "PPG Noise Reduction Based on Adaptive Frequency Suppression Using Discrete Fourier Transform for Portable Home Monitoring Applications," in 2018 15th IEEE India Council International Conference (INDICON)), Coimbatore, India, December 16–18, 2018, 1–6. doi:10.1109/INDICON45594.2018.8987004

Safieddine, D., Kachenoura, A., Albera, L., Birot, G., Karfoul, A., Pasnicu, A., et al. (2012). Removal of Muscle Artifact from EEG Data: Comparison between Stochastic (ICA and CCA) and Deterministic (EMD and Wavelet-Based) Approaches. *EURASIP J. Adv. Signal Process.* 2012, 127. doi:10.1186/1687-6180-2012-127

Schönle, P., Schulthess, F., Fateh, S., Ulrich, R., Huang, F., Burger, T., et al. (2013). "A DC-connectable Multi-Channel Biomedical Data Acquisition ASIC with Mains Frequency Cancellation," in 2013 Proceedings of the ESSCIRC (ESSCIRC), Bucharest, Romania, September 16–20, 2013, 149–152. doi:10.1109/ESSCIRC.2013.6649094

Seo, G., Lee, G., Kim, M. J., Baek, S.-H., Choi, M., Ku, K. B., et al. (2020). Rapid Detection of COVID-19 Causative Virus (SARS-CoV-2) in Human Nasopharyngeal Swab Specimens Using Field-Effect Transistor-Based Biosensor. *ACS Nano* 14, 5135–5142. doi:10.1021/acsnano.0c02823

Shad, E. H. T., Molinas, M., and Ytterdal, T. (2020). Impedance and Noise of Passive and Active Dry EEG Electrodes: A Review. *IEEE Sensors J.* 20, 14565–14577. doi:10.1109/jsen.2020.3012394

Shaltis, P. (2008). A Wearable Blood Pressure Sensor Using Oscillometric Photoplethysmography and Micro Accelerometers. Ph.D. thesis. Cambridge (MA): Massachusetts Institute of Technology.

Shan, B., Broza, Y. Y., Li, W., Wang, Y., Wu, S., Liu, Z., et al. (2020). Multiplexed Nanomaterial-Based Sensor Array for Detection of COVID-19 in Exhaled Breath. *ACS Nano* 14, 12125–12132. doi:10.1021/acsnano.0c05657

Song, J., Shan, T., Zhu, S., and Chiu, Y. (2014). "A Motion-Artifact Tracking and Compensation Technique for Dry-Contact EEG Monitoring System," in 2014 IEEE Signal Processing in Medicine and Biology Symposium (SPMB), Pennsylvania, PA, December 13, 2014, 1–4. doi:10.1109/SPMB.2014.7002951

Song, H., Park, Y., Kim, H., and Ko, H. (2015). Fully Integrated Biopotential Acquisition Analog Front-End IC. *Sensors* 15, 25139–25156. doi:10.3390/s151025139

Taheri, B. A., Knight, R. T., and Smith, R. L. (1994). A Dry Electrode for EEG Recording. *Electroencephalography Clin. Neurophysiol.* 90, 376–383. doi:10.1016/0013-4694(94)90053-1

Tamura, T., Maeda, Y., Sekine, M., and Yoshida, M. (2014). Wearable Photoplethysmographic Sensors-Past and Present. *Electronics* 3, 282–302. doi:10.3390/electronics3020282

Teplan, M. (2002). Fundamentals of EEG Measurement. *Measure. Sci. Review* 2, 1–11.

Utami, N., Setiawan, A. W., Zakaria, H., Mengko, T. R., and Mengko, R. (2013). "Extracting Blood Flow Parameters from Photoplethysmograph Signals: A Review," in 2013 3rd International Conference on Instrumentation, Communications, Information Technology and Biomedical Engineering (ICICI-BME), Bandung, Indonesia, (New York, NY, United States), 403–407. doi:10.1109/ICICI-BME.2013.6698535

Wahoo Fitness (2021). Wahoo Fitness (TICKR). Available at: https://www.wahoofitness.com/devices/heart-rate-monitors.

Wang, F., Li, G., Chen, J., Duan, Y., and Zhang, D. (2016). Novel Semi-dry Electrodes for Brain–Computer Interface Applications. *J. Neural Eng.* 13, 046021. doi:10.1088/1741-2560/13/4/046021

Webster, J. G. (2009). *Medical Instrumentation: Application and Design*. Hoboken, NJ: John Wiley & Sons.

Woestenburg, J. C., Verbaten, M. N., and Slangen, J. L. (1983). The Removal of the Eye-Movement Artifact from the EEG by Regression Analysis in the Frequency Domain. *Biol. Psychol.* 16, 127–147. doi:10.1016/0301-0511(83)90059-5

Wolling, F., Heimes, S., and Van Laerhoven, K. (2019). Unity in Diversity: Sampling Strategies in Wearable Photoplethysmography. *IEEE Pervasive Comput.* 18, 63–69. doi:10.1109/MPRV.2019.2926613

Wolpaw, J. R., Birbaumer, N., McFarland, D. J., Pfurtscheller, G., and Vaughan, T. M. (2002). Brain–computer Interfaces for Communication and Control. *Clin. Neurophysiol.* 113, 767–791. doi:10.1016/S1388-2457(02)00057-3

Xu, J., and Zhong, B. (2018). Review on Portable EEG Technology in Educational Research. *Comput. Hum. Behav.* 81, 340–349. doi:10.1016/j.chb.2017.12.037

Xu, J., Yazicioglu, R. F., Grundlehner, B., Harpe, P., Makinwa, K. A. A., and Van Hoof, C. (2011). A 160 μ*W* 8-Channel Active Electrode System for EEG Monitoring. *I*EEE Trans. Biomed. Circuits Syst. 5, 555–567. doi:10.1109/tbcas.2011.2170985

Xu, J., Mitra, S., Van Hoof, C., Yazicioglu, R. F., and Makinwa, K. A. A. (2017). Active Electrodes for Wearable EEG Acquisition: Review and Electronics Design Methodology. *IEEE Rev. Biomed. Eng.* 10, 187–198. doi:10.1109/rbme.2017.2656388

Xu, K., Jiang, X., and Chen, W. (2020). Photoplethysmography Motion Artifacts Removal Based on Signal-Noise Interaction Modeling Utilizing Envelope Filtering and Time-Delay Neural Network. *IEEE Sensors J.* 20, 3732–3744. doi:10.1109/JSEN.2019.2960370

Yang, Yi-Hsiang., and Tang, Kea-Tiong. (2014). "A Pulse Oximetry System with Motion Artifact Reduction Based on Fourier Analysis," in 2014 IEEE International Symposium on Bioelectronics and Bioinformatics (IEEE ISBB), Chung Li, Taiwan, January 01, 2014, 1–4. doi:10.1109/ISBB.2014.6820902

Yang, D., Cheng, Y., Zhu, J., Xue, D., Abt, G., Ye, H., et al. (2018). A Novel Adaptive Spectrum Noise Cancellation Approach for Enhancing Heartbeat Rate Monitoring in a Wearable Device. *IEEE Access* 6, 8364–8375. doi:10.1109/ACCESS.2018.2805223

Yao, Jianchu., and Warren, S. (2005). "A Short Study to Assess the Potential of Independent Component Analysis for Motion Artifact Separation in Wearable Pulse Oximeter Signals," in 2005 IEEE Engineering in Medicine and Biology 27th Annual Conference, Shanghai, China, September 1–4, 2005. 3585–3588. doi:10.1109/IEMBS.2005.1617256

Yin, M., and Ghovanloo, M. (2007). A Low-Noise Preamplifier with Adjustable Gain and Bandwidth for Biopotential Recording Applications. *IEEE Int. Symp. Circuits Syst.* 321–324. doi:10.1109/ISCAS.2007.378400

Yousefi, T., Dabbaghian, A., and Kassiri, H. (2020). "Motion-Affected Electrode-Tissue Interface Characterization for Ambulatory EEG Recording," in 2020 42nd Annual International Conference of the IEEE Engineering in Medicine & Biology Society (EMBC), Montreal, QC, July 20–24, 2020 (IEEE), 4479–4482. doi:10.1109/embc44109.2020.9176671

Zhang, H., Sun, Y., Lu, Y., Lan, J., and Ji, Y. (2015). "A Novel Motion and Noise Artifacts Reduction Mechanism (MNARM) for Wearable PPG-Based Heart Rate Extraction," in 2015 IET International Conference on Biomedical Image and Signal Processing (ICBISP), Beijing, China, November 19, 2015, 1–4. doi:10.1049/cp.2015.0785

Zhao, H., Liu, F., Xie, W., Zhou, T.-C., OuYang, J., Jin, L., et al. (2021). Ultrasensitive Supersandwich-type Electrochemical Sensor for SARS-CoV-2 from the Infected COVID-19 Patients Using a Smartphone. *Sensors Actuators B: Chem.* 327, 128899. doi:10.1016/j.snb.2020.128899

Zhou, X., Li, Q., Kilsgaard, S., Moradi, F., Kappel, S. L., and Kidmose, P. (2016). "A Wearable Ear-EEG Recording System Based on Dry-Contact Active Electrodes," in 2016 IEEE Symposium on VLSI Circuits (VLSI-Circuits), May 24, 2016, 1–2. doi:10.1109/VLSIC.2016.7573559

Zhu, S., Tan, K., Zhang, X., Liu, Z., and Liu, B. (2015). "MICROST: A Mixed Approach for Heart Rate Monitoring during Intensive Physical Exercise Using Wrist-type PPG Signals," in 2015 37th Annual International Conference of the IEEE Engineering in Medicine and Biology Society, Milan, Italy, March 15, 2015 (New York, NY, United States: EMBC), 2347–2350. doi:10.1109/EMBC.2015.7318864

Zou, X., Xu, X., Tan, J., Yao, L., and Lian, Y. (2008). "A 1-V 1.1-μW Sensor Interface IC for Wearable Biomedical Devices," in 2008 IEEE International Symposium on Circuits and Systems, Seattle, Wa, May 18–21, 2008, 2725–2728. doi:10.1109/ISCAS.2008.4542020

Conflict of Interest: The authors declare that the research was conducted in the absence of any commercial or financial relationships that could be construed as a potential conflict of interest.